Carbohydrate Polymer Technologies and Applications 9 (2025) 100730

Contents lists available at ScienceDirect

Carbohydrate Polymer Technologies and Applications

journal homepage: www.sciencedirect.com/journal/carbohydrate-polymer-technologies-and-applications

Microwave assisted extraction of chitosan from *Agaricus bisporus*: techno-functional and microstructural properties

Adity Bahndral [a], Rafeeya Shams [a,*], Kshirod Kumar Dash [b,*], Pintu Chaudhary [c], Ayaz Mukarram Shaikh [d], Kovács Béla [d,*]

[a] Department of Food Technology and Nutrition, Lovely Professional University, Phagwara, Punjab, India
[b] Department of Food Engineering and Technology, Ghani Khan Choudhury Institute of Engineering and Technology, Malda, West Bengal, India
[c] Department Department of Food Technology, C.B.L. Government Polytechnic, Bhiwani, Haryana, India
[d] Faculty of Agriculture, Food Science and Environmental Management Institute of Food Science, University of Debrecen, Debrecen 4032, Hungary

ARTICLE INFO

Keywords:
Agaricus bisporus
Antioxidant activity
Chitosan
Crystallinity index
Degree of deacetylation
Microwave irradiation

ABSTRACT

Chitosan, a copolymer of glucosamine and N-acetyl glucosamine, is primarily derived from chitin. The present research was conducted to generate and analyze chitosan derived from white button mushroom waste (*Agaricus bisporus*) using microwave assisted extraction. Dried mushroom waste powder was demineralized in diluted acid using 3 M HCl in 1:10 w/v at 540 W for 8 min and deproteinated at 180 W using 10% NaOH in 1:10 w/v for 8 min to remove proteins and lipids. The extracted chitin was deacetylated using 50% NaOH in 1:20 w/v at 360 W to convert it into chitosan. Chitin from the aforesaid process was deacetylated in concentrated alkaline medium at 360 W for 8 min to yield chitosan by converting acetyl groups to -NH_2 groups. The pH and solubility of fresh chitosan were 7.5 and 75%, respectively. Extracted chitosan had maximum 2,2-diphenyl-1-picrylhydrazyl (DPPH) free radical scavenging activity of 53.97% and reducing power of 3.58. The microwave irradiation method produced chitosan having degree of deacetylation of 79.94% and crystallinity index of 1.09. The spectra bands confirmed existence of NH_2, OH, C—O, CH, and C—N functional groups. The X-ray diffraction analysis of the chitosan sample discovered distinct peaks at 2θ values between 10 and 20 °, indicating its semi-crystalline nature.

1. Introduction

The consumption of mushrooms has significantly expanded in recent years because of its high nutritional value and health benefits, which are attributed to the presence of proteins, vitamins, minerals, fungal polysaccharides (particularly β-glucans), and antioxidants. Around 20 of the more than 35 edible mushroom species that are commercially grown worldwide are produced on an industrial basis (Pandey et al., 2024; Silva et al., 2024). Among them *Agaricus bisporus* is one of the most often consumed mushrooms worldwide (Siwulski et al., 2020). Mushrooms, which belong to the fungi kingdom, offer substantial nutritional benefits, with approximately 2000 edible species found globally (El Sheikha, 2022). Among these, the most commonly grown varieties comprise the button mushroom (*Agaricus bisporus*), oyster mushrooms (*Pleurotus spp.*), and shiitake mushroom (*Lentinula edodes*). In 2018, the worldwide market worth of farm fresh mushrooms stood at 38 billion USD, with China emerging as the dominant mushroom grower in Asia, making up about 35% of the total global mushroom market share, as reported by Bhagarathi et al. (2023). Asia countries subsidize maximum mushroom production up to 76%, here after by Europe (17.2 %) and United States (5.9 %) (Yadav et al., 2021). India exhibits diverse agro-climatic conditions and is primarily an agrarian nation, utilizing roughly 4.37% of its land for cultivation and producing approximately 620 million tons of agricultural waste each year. In particular, the market for *Agaricus bisporus,* or white mushrooms, was worth USD 16.73 billion in 2020 and is projected to grow to USD 27.39 billion by 2028 (Zion Market Research, 2021). India has the potential to generate 3 million tonnes of mushrooms and approximately 15 million tonnes of bio-compost from agricultural waste in context regarding mushroom cultivation (Raman et al., 2018). Currently, industries encounter losses linked to the safe disposal of mushroom waste, including mushroom stems and misshapen mushrooms whose size or shape do not meet commercial standards contributing to the final production costs of products (Papoutsis et al., 2020). Adopting a value-addition approach has the potential to generate extra

* Corresponding authors.
E-mail addresses: rafiya.shams@gmail.com (R. Shams), kshirod@tezu.ernet.in (K.K. Dash), kovacsb@agr.unideb.hu (K. Béla).

https://doi.org/10.1016/j.carpta.2025.100730

Available online 24 February 2025

revenues for industries while simultaneously reducing the costs associated with the primary biotechnological product (Singh & Thakur, 2023). Unfortunately, the rapid expansion in industrial edible mushroom production has resulted in massive amounts of mushroom waste each year, notably mushroom stems and deformed mushrooms whose size or shape do not satisfy commercial standards. As a result, current academic and commercial interest in mushroom waste is increasingly focused on its valorisation in order to fulfil the quest of circular economy and sustainability principles (Pérez-Bassart et al., 2023). Mushroom stems and discards contain chitin and β-glucans, which could be used to create biodegradable products. This is a highly underexplored field, with potential interest in shifting the food packaging business towards environmentally friendly packaging solutions to develop bio-based and biodegradable polymers (Feng et al., 2022). The practice of growing mushrooms not only plays a role in recycling agricultural waste but also addresses the nutritional deficiencies prevalent among a significant portion of the Indian population (Thakur, 2020). Furthermore, this approach will bolster the economy and contribute to mitigating environmental pollution.

Edible mushrooms, comprising primarily of chitin, glucans, and proteins within their cell walls, serve as a valuable dietary fiber source. Dietary fiber holds significance as a functional component in food, employed for purposes such as food swelling, thickening, film formation, stabilization, and overall contributing as a crucial health-enhancing ingredient. Hence, the dietary fibers derived from chitin prove beneficial in enhancing functional foods, as highlighted by González et al. (2020). Chitin, a natural substance present in the outer skeletons of most marine creatures also in an outer cellular wall of fungi and yeasts, holds considerable importance in this context. Glucosamine, an essential predecessor of proteins and lipids in living systems, acts as the fundamental backbone of chitin. Glucosamine linkage units occurs via β 1–4 glycosidic bond, as explained by Cummings (2024). Structurally, chitin bears resemblance to cellulose, with the distinction having hydroxyl (OH) group present in cellulose is substituted by an acetyl amine ($NHCOCH_3$) group (Rahangdale et al., 2019). The efficacy of chitin is heavily swayed by the quantity and proportion of n-acetylated units. "Degree of acetylation (DA)" term refers to the count of n-acetylated units in a macro molecule, while "degree of deacetylation (DD)" term denotes the number of these units within bio polymer, as explained (Wattjes et al., 2020). Despite its widespread presence in environment, the potential utilization of chitin in food industry poses certain challenges. These challenges stem mainly from its resistance to dissolution in certain commonly used solvents and its limited biodegradability.

The physicochemical characteristics of chitin, such as high crystallinity, acetamido content, and the hydrogen bonds present between its carbonyl and hydroxyl groups, contribute to these limitations (Korampattu et al., 2024). As a solution to these challenges, chitin undergoes deacetylation to yield chitosan. Chitosan, distinguished by improved solubility compared to chitin, along with notable bacteriostatic, antimicrobial, biocompatible, and biodegradable properties, stands out as a significant biopolymer. The beneficial features of chitosan proves it a vital biological element with diverse implementations across the food production outlets (Shoueir et al., 2021; Zhan et al., 2024). Traditionally, extracting chitosan involved methods that has require extended heating periods, making the process lengthy—often taking several hours or even days—and consuming a significant amount of energy (Hisham et al., 2024). To address these difficulties, it is essential to explore alternative extraction methods that are quick, efficient, and eco-friendly. Microwave technology-based extraction methods effectively fulfill these criteria (Liaqat et al., 2023). Unlike traditional extraction methods, microwave synthesis greatly shortens reaction times and improves both yield and product purity by reducing unwanted side reactions (Da Costa et al., 2023). In the last ten years, microwave irradiation has become a commonly employed and powerful method for quickly and effectively synthesizing a range of substances (Cheng et al., 2020). It is a crucial process for accelerating the synthesis of both inorganic and organic compounds, applicable across various fields of chemistry (Abolhasani & Kumacheva, 2023). This innovative technology has supplanted traditional heating methods heating of the reaction mixture by utilizing three-dimensional. It facilitates chemical changes within minutes, a notable enhancement compared to the hours or days typically needed with conventional approaches (Banik et al., 2021).

Microwaves do not directly generate heat; instead, they induce heat indirectly through a process known as dielectric heating. Microwave ovens utilize microwaves, a type of electromagnetic radiation, to stimulate the water molecules, lipids, and sugars found in food. These substances display electric dipole moments, suggesting the existence of separate positive and negative charges within the molecule. The molecules align with the electric field due to the fast oscillation of the microwaves. These structural changes occur as the frequency changes, influenced by an alternating electric field. The molecules, once excited, undergo rapid movement, and the resulting friction from these movements generates heat (Hu et al., 2021). (Mahdy, 2019) utilized microwave emission application for extraction of chitosan, particularly for deacetylation process of chitin. Chitosan's distinctive properties have led to a rapid expansion of its applications across various domains (Abdel-Gawad et al., 2017; Dai et al., 2023; Duan et al., 2023; Yu et al., 2023). Considering chitosan versatility particularly in the fields of food manufacturing and healthcare, arises from its ability to degrade naturally, its compatibility with living organisms, not having any of toxicity, its ability to provide protection against microorganisms, its potential to combat tumours, and its ability to improve tumour treatment (Aranaz et al., 2021; Manna et al., 2023; Khubiev et al., 2023; Kritchenkov et al., 2020; Abourehab et al., 2022; Thirugnanasambandan & Gopinath, 2023) Microwave-assisted chitosan extraction provides numerous benefits, including faster deacetylation and lower energy consumption. However, it also has its limitations. The main drawback of microwave-assisted extraction is its limited ability to produce fungal chitosan biomass. Therefore, more efficient extraction techniques are required to maximize chitosan yield from the available biomass (Sebastian et al., 2019). While microwave-assisted extraction reduces energy consumption and has a lower environmental footprint, it is crucial to consider its overall environmental impact. Other environmentally friendly extraction methods might offer greater sustainability. The selection of an extraction method depends on factors such as resource availability and cost. Although microwave-assisted extraction is efficient, it may not always be the most economical choice (Egorov et al., 2023). Therefore, this work is aimed to evaluated the optimum conditions suitable for one of the most cultivated mushroom (*Agaricus bisporus*) waste for extracting chitin by mean of microwave assisted demineralization and deproteination followed by conversion of chitin into chitosan by mean of microwave assisted deacetylation and to investigate the characteristic properties of the extracted chitosan. The intent of this research was to extract chitosan from mushroom waste, which has been particularly challenging in current times as a result of difficulty in achieving peculiarities comparable to those of fully synthetic products, as fishery wastes and crustacean waste are the most useful source for chitosan extraction therefore by employing microwave treatment during extraction minimizes the time required additionally, the techno-functional characteristics and characterization of the extricated chitosan were evaluated.

2. Material and methods

2.1. Materials

Standard sodium hydroxide pellets (NaOH) ≥98% and hydrochloric acid (HCl) 37% were obtained from Sigma-Aldrich (Sigma-Aldrich, St. Louis, MI, USA). All reagents utilized were of high purity grades, and double distilled water was employed to prepare aqueous solutions.

2.2. Preparation of raw material

The byproducts of white button mushrooms (*Agaricus bisporus*) were acquired from Randhawa mushroom farm located in Batala, Punjab, India, on the same day as the mushroom harvest. The mushrooms were of medium size, with cap diameters typically falling between 3 and 4.5 cm. Every batch of mushrooms was harvested in the morning by skilled workers. The mushroom stalks were gathered by removing the mycelium from the bases of the stalks. After one day of harvesting, the stalks were washed, cut into pieces and stored overnight at 5 ± 2 °C. To produce mushroom waste powder (MWP), 3 kg of mushroom stalks *(Agaricus bisporous)* were arranged on trays made of stainless steel and exposed to sun drying. The ambient temperature varied between 25±5 °C, with a relative humidity of 40 % over a period of around 3 days, with an average daily exposure time of 9 to 10 h. The dried slices were pulverized to permeate a sieve with 80 mesh openings, leading to MWP (Fig. 1). To eliminate any remaining vapour, if existing, MWP was made susceptible to drying by domestic microwave oven (Model IFB 30BRC2, India) at 45±2 °C unless reached a stable weight, following the process defined by Maray et al. (2018). The initial and final moisture contents of the samples were measured with a moisture analyzer (MB 25, Ohaus Corporation, Parsippany, NJ, USA) with an accuracy of 0.001%. After drying, 450*g* of powder was collected, with an average yield of mushroom waste powder of 15.0% which was then packed in low-density polyethylene (LDPE) and kept in a refrigerator at 4 ± 2 °C prior the study was completed.

2.3. Methodology for isolation of chitosan from mushroom waste powder (MWP)

The extraction of chitosan from MWP was accomplished using three sequential steps: Demineralization, deproteinization, and deacetylation, each carried out for a fixed duration of 8 min (El Knidri et al., 2016). Demineralization was conducted in a glass beaker positioned within domestic microwave oven (Model IFB 30BRC2, India). 10*g* of powdered sample was treated with a solution of 3 M HCl at a ratio of 1:10 (sample to solvent) and heated for 8 min at various power levels (as shown in table 1), Subsequently, the mixture was filtrated and rinse off three times using distilled water prior being dried at 40±2 °C temperature. For deproteinization, the sample was poured in glass beaker within a home held microwave oven (Model IFB 30BRC2, India). Then it was blended with a 10% NaOH solution at 1:10 ratio (sample to solvent) and heated for 8 min at various power levels, as indicated in Table 1. Subsequently, the solution was filter out and wash off three times with distilled water before being dried at 40±2 °C temperature. Deacetylation was conducted in a glass beaker within a domestic microwave oven (Model IFB 30BRC2, India). Sample was mixed with a 50% NaOH solution at 1:20 ratio (sample to solvent) and heated for 8 min at various power levels as shown in Fig. 2. However, the chitosan was extracted from MWP using conventional method, as outlined in Table 1. For demineralization, 10*g* of MWP was treated with a 1 M HCl aqueous solution at a 1:15 solid-to-solution ratio. This process took place in a water bath shaker (Memmert GmbH, Wisconsin, USA) at 30 ± 2 °C, with continuous stirring in at 200 rpm for 2 h to eliminate calcium carbonate and other calcium salts (Omer et al., 2019). Subsequently, for deproteination, the extract was treated with a 1 M sodium hydroxide solution at a 1:15 w/v ratio as depicted in Fig. 3. This mixture was then refluxed using magnetic stirrer with hot plate (Model DBK 30MAG12D, India) (at 90±2 °C for 2 h to remove proteins and fats (Omer et al., 2019). The extracted chitin was then deacetylated using a 60 wt% NaOH aqueous solution at a 1:15 w/v ratio. This process was conducted in a 100±2 °C water bath with agitation (Model SI- SWB/30LTPID Microprocessor, India) at 200 rpm for 8 h. Afterwards, the mixture was strained and thoroughly washed with deionized water before being dried at a temperature of 40 ±2 °C. The extracted chitosan was packed in low-density polyethylene (LDPE) and kept in a refrigerator at 4 ± 2 °C prior the study was completed.

Table 1
Treatment details for the extraction of chitosan from mushroom waste powder using different extraction techniques.

Treatment	Demineralization (8 min; 3 M HCl; 1:10 w/v)	Deproteination (8 min; 10% NaOH; 1:10 w/v)	Deacetylation (8 min; 50% NaOH; 1:20 w/v)
T1	360W	180W	360W
T2	360W	180W	540 W
T3	360W	360W	360W
T4	360W	360W	540W
T5	540W	180W	360W
T6	540W	180W	540W
T7	540W	360W	360W
T8	540W	360W	540W
T0 (Conventional extraction method)	2 hr; 1 M HCl (1:15 w/v) at 30 °C ± 5	2hr; 1 M NaOH (1:15 w/v) at 90 °C ± 5	8 hr; 60% NaOH (1:15 w/v) at 100 °C ± 5

W=Watt; *M*=Molar.

2.4. Techno-functional properties of extracted chitosan powder

2.3.1. Yield of extracted chitosan powder

The amount of chitosan prepared was evaluated and yield was measured employing Eq. (1) (Agarwal et al., 2018).

$$\% \text{ Yield} = \frac{\textit{Practical yield}}{\textit{Theoritical yield}} \times 100 \quad (1)$$

2.3.2. pH and solubility of extracted chitosan powder

pH of the cellulose solution was determined through a pH meter (LT-50 microprocessor pH meter, India) by placing a 5*g* sample into a clean and dry 150 ml beaker holding 40 ml of deionized water, stirring, and centrifuging for 5 min using centrifuge (REMI R-02, mini centrifuge, India), the pH of the supernatant was assessed. Chitosan powder (0.2 g)

Fig. 1. **[A]** Fresh raw button mushroom waste **[B]** the paste of button mushroom waste prior to drying and **[C]** Mushroom waste powder after drying.

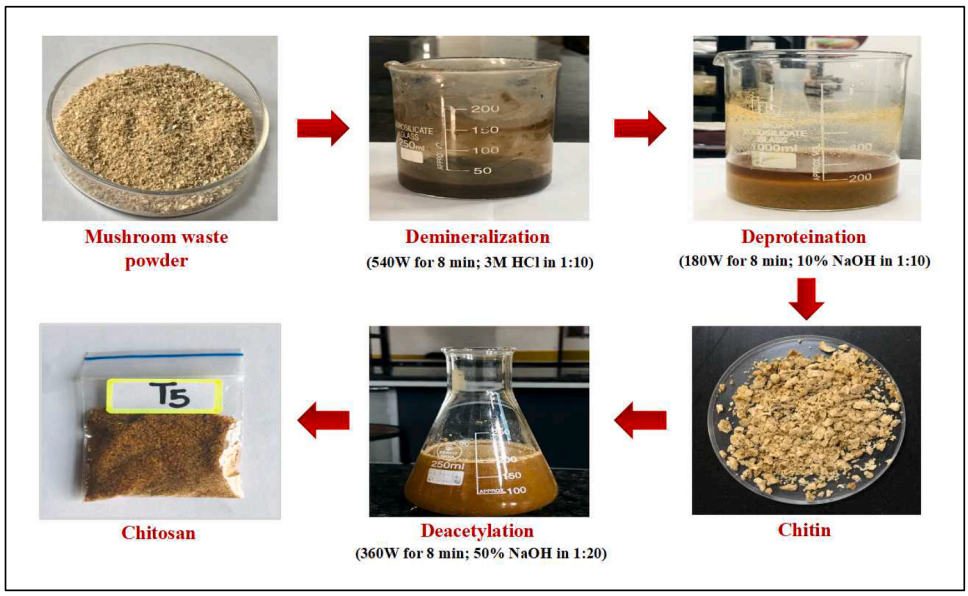

Fig. 2. Detailed steps involved in microwave assisted extraction of chitosan from mushroom waste powder.

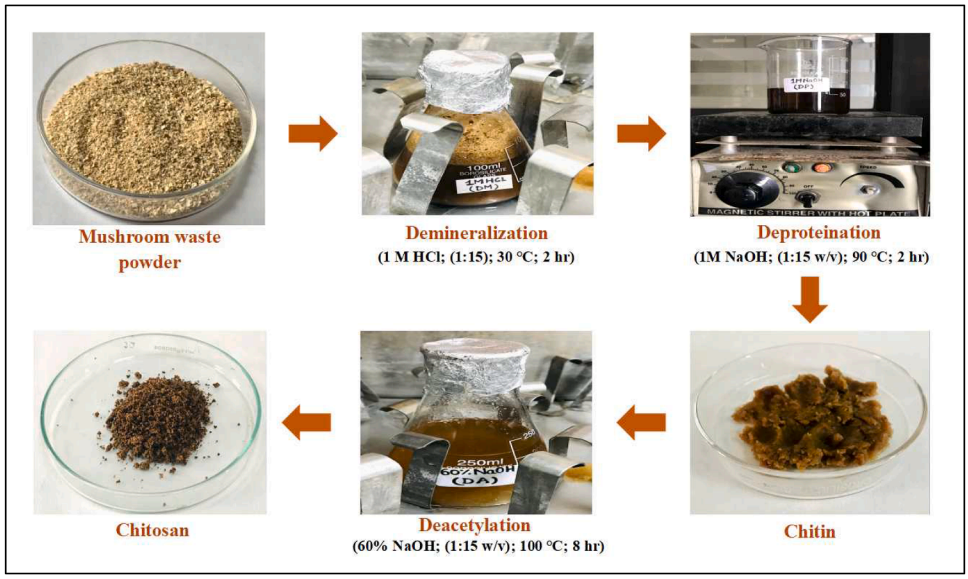

Fig. 3. Detailed steps involved in Traditional extraction of chitosan from mushroom waste powder.

excerpted was blended in a 20-mL solution of 1% acetic acid in beaker. This mixture was then blent on a magnetic stirrer (REMI 2 MLH magnetic stirrer, India) at 250 rpm for 30 min at 25 °C temperature. Then, solution was strained using a Millipore 20 μ nylon membrane filtration assembly. Insoluble portion is known as the retardant, accumulated on membrane filter, was rinsed using distilled water. The percentage solubility of chitosan was measured using equation (2) (Agarwal et al., 2018).

$$\text{Solubility\%} = 100 - \left[\frac{\textit{Weight of insoluble fraction}}{\textit{Initial weight of the sample}}\right] \times 100 \quad (2)$$

2.3.3. Bulk density, tapped density, Hasneur ratio and Carr's index of chitosan powder

Take 1 g chitosan powder and pour into 10 ml measuring cylinder without tapping, record its bulk density and expressed in grams per milliliter (g/ml). To determine the tapped density, take 1 g chitosan powder and deposit into 10 ml measuring cylinder, mildly patt the cylinder for a duration of 2 min. Ratio of tapped density to bulk density indicate flowability and is referred to as the Hasneur ratio, as defined by the Eq. (3) (Jindal et al., 2013).

$$\text{Hasneur ratio} = \frac{\text{Tapped density (mg/ml)}}{\text{Bulk density (mg/ml)}} \quad (3)$$

Carr's index is the measure of compressibility and is evaluated using Eq. (4).

$$\text{Carr's index \%} = \frac{\text{Tapped density (mg/ml)} - \text{bulk density (mg/ml)}}{\text{Tapped density (mg/ml)}} \times 100 \quad (4)$$

2.3.4. Degree of deacetylation (DD) of extracted chitosan powder

The infrared spectroscopy (IR) technique was employed to measure the DD of chitosan. The baseline for calculating the DD was established

accordingly described by Zhang et al. (2012) and the computational equation is presented in Eq. (5).

$$DD = 100 - \left[\frac{A1655}{A3450} \times 100\right] \Big/ 1.33 \quad (5)$$

Where A1665 and A3450 represent the absorbance values at 1655 cm^{-1} for the amide-I band, indicative of the N-acetyl group content, and at 3450 cm^{-1} for the hydroxyl band, used as an internal standard to adjust the thickness of the film or variations in concentration of chitosan powder. Factor '1.33′ represents ratio of A1665/A3450 for fully N-acetylated chitosan presuming that for complete deacetylated chitosan the ratio had a value of zero.

2.3.5. Crystallinity

Crystallinity index of chitosan powder was additionally assessed through FTIR analysis using a Perkin Elmer instrument (Spectrum 100, PerkinElmer, USA). Formula for computing crystallinity is provided in Eq. (6) (Agarwal et al., 2018).

$$CI = \frac{A1379}{A2929} \quad (6)$$

Where, A1379 and A2929 are the absorbance at 1379 cm^{-1} and 2929 cm^{-1}

2.3.6. Antioxidant activity (AA)

Scavenging activity of chitosan on 1,1-diphenyl-2-picrylhydrazyl (DPPH) radicals (D4313-TCI America) was evaluated using a modified method from Pasanphan et al. (2015). Chitosan samples (ranging from 0.125 to 1.0 mg/ml) in 0.2% solution of acetic acid (A9705-Sigma-Aldrich) were admixed with 1 ml of a methanolic DPPH solution, resulting in ultimate DPPH concentration of 1.0 mM. Mixture was then vigorously agitated and allowed to sit in the dark for 30 min, after which absorbance was recorded at 517 nm relative to blank. Ascorbic acid (PHR1008-Sigma-Aldrich) served as the reference standard. Scavenging capacity was then computed using formula below:

$$AA\ \% = \frac{A517\ \text{of control} - A517\ \text{of sample}}{A517\ \text{of control}} \times 100 \quad (7)$$

2.3.6.1. Reducing power assay (RP). The reducing power (RP) was assessed following the method of (Pasanphan et al., 2015). Chitosan samples (0.125 to 1.0 mg/ml) were combined with 2.5 ml of phosphate buffer (0.2 M, pH 6.6) (76,847-Sigma-Aldrich) and 2.5 ml of 1% potassium ferricyanide (P1979- TCI America). Reaction mixture was incubated in a water bath (STXUWB25, India) at 50 °C for 20 min. Following incubation, 2.5 ml of 10% trichloroacetic acid (T6399-Sigma-Aldrich) was appended, then the centrifugation of the mixture was completed at 3000 rpm for 10 min using centrifuge (REMI R-02, mini centrifuge, India). 2.5 ml of the solution from upper layer was combined with 2.5 ml of deionized water and 0.5 ml of 0.1% ferric chloride (157,740-Sigma-Aldrich). The absorbance of the resulting solution was recorded at 700 nm, with rise in absorbance indicating higher reducing power.

2.3.7. Fourier transform infrared spectroscopy (FTIR)

FTIR study of prepared chitosan powder was measured to detect and recognize the appearance of functional groups, components and nature of bonding. Various samples were analyzed using a Perkin Elmer instrument (Spectrum 100, PerkinElmer, USA) having resolution of 4 cm^{-1} within 4000 to 400 cm^{-1} range (Liu et al., 2013).

2.3.8. X-ray powder diffractometry (XRD)

XRD analysis of obtained chitosan powder was carried out with EcoX-ray diffractometer (Deutsch D8 Advance ECO-Bruker). Particle size was controlled to be up to 200 μm and diffraction pattern was examined by means of Cu-Kα radiation with a wavelength of 1.54 Å, covering angle ranges from 5° to 50° (Agarwal et al., 2018).

2.3.9. Thermogravimetric analysis (TGA)

Thermal stability of the samples was assessed utilizing a Thermogravimetric Analyzer (Q5000 series, TA Instruments, USA). Approximately sample of 10 mg were heated in open alumina pans, under a helium atmosphere, starting at 30 °C up to approximately 800 °C with 10 °C/min heating rate. % moisture content was measured from the TGA thermogram using TA Universal Analysis software (Hassainia et al., 2018).

2.3.10. Differential scanning calorimetry (DSC)

Thermal property of cellulose samples was analyzed through Differential Scanning Calorimeter (DSC), model SDT Q600 from TA Instruments. Samples were weighed and laid in hermetic pans and subjected to heating at 25 °C up to 700 °C at a rate of 5 °C/min Gichuki et al. (2022).

2.3.11. Statistical analysis

All experiments were conducted in triplicates. The results were presented as mean ± standard deviation. SPSS software (version 16.0, IBM, Chicago, IL, USA) was used to carry out statistical analyses. Mean values were considered significant at 95% confidence level ($p < 0.05$).

3. Result and discussion

3.1. Yield and moisture content

The techno functional nature of chitosan powder obtained from different treatments at varied power levels were pictured in Fig. 4, in following Table 2 all the corresponding values are summarized. Chitosan was effectively obtained by the deacetylation process of mushroom chitin. The quality and techno-functional characteristics of prepared chitosan can significantly alter relying on quality of mushroom chitosan and the methods employed in its preparation. The fraction yield of chitosan obtained ranged from 6.18± 0.02% to 6.98± 0.10%. This variance can be attributed during the deproteination process where reduction in the acetyl group from chitin was seen when undiluted alkali (NaOH) solution was used, as explained by Agarwal et al. (2018). (Boureghda et al., 2021) reported similar results when extracting chitin from various segments of *A. bisporous* (Stipe and gills), yielding 7.4% and 5.9%, respectively, using acetic acid. In a parallel study investigating the amount of chitin of the pileus and stipes of mushroom at various growth stages of *A. bisporus, Lentinula edodes*, and *Pleurotus ostreatus,* the influence of the growing stage was examined, (Vetter, 2007) found that *A. bisporus* exhibited the highest chitin levels ie., 6.94 to 7.84% using acid (HCl) for extraction, Moreover, the entire fruit body yielded even higher, reaching up to 8.68%. The moisture percentage after extraction of chitosan under various conditions was assessed, and the corresponding values are presented in Table 2. The moisture percentage was obtained in T5 i.e., 6.01±0.08% and the yield obtained to the respective treatment is 6.98±0.10%, whereas the yield and moisture content for T0 (using traditional extraction technique) was obtained to be 6.09±0.01% and 5.75±0.03% respectively. Moisture content plays a crucial role as it can influence the strength of strong NaOH needed during the deacetylation process. Thus, this might weaken the effectiveness of removing acetyl groups from chitin, accordingly affecting overall DD of end product shown by Novikov et al. (2023). (Malm, 2021) and (Ibitoye et al., 2018) extracted chitosan from grasshoppers and house crickets, achieving maximum yields of 5.7% and 5.8%, respectively, using traditional extraction methods throughout the extraction process. The reason for reduced mass loss primarily attributed to the removal of proteins and minerals during deproteinization and demineralization processes (Da Silva Lucas et al., 2021). As reported, inadequate HCl concentration in traditional methods may result in reduced yields of ultrapure chitin. Conversely, excess acid may accelerate the

Fig. 4. Chitosan powder extracted from mushroom waste powder using microwave assisted extraction technique.

Table 2
Techno-functional properties of prepared chitosan samples.

S. No.	Chitosan sample	% Moisture	% Yield	pH	% Solubility	Bulk density (g/ml)	Tapped density (g/ml)	Carr's index	Hasneur ratio
	T0	5.75±0.03^{d}	6.09±0.01^{c}	6.6 ± 0.01^{a}	59.04±0.03^{a}	0.67±0.04^{b}	0.83±0.02^{d}	19.27±0.04^{c}	1.24±0.03^{a}
2.	T1	7.21±0.13^{a}	6.65±0.11^{a}	6.7 ± 0.1^{a}	60.45±0.11^{a}	0.74±0.01^{a}	0.89±0.01^{a}	16.85±0.15^{a}	1.20±0.01^{a}
3.	T2	7.12±0.11^{a}	6.56±0.09^{a}	6.5 ± 0.2^{a}	60.39±0.12^{a}	0.73±0.01^{a}	0.85±0.007^{b}	14.11±0.81^{b}	1.16±0.01^{b}
4.	T3	7.86±0.04^{b}	6.26±0.03^{b}	7.0 ± 0.2^{b}	70.19±0.29^{b}	0.71±0.01^{b}	0.86±0.002^{c}	17.44±0.14^{c}	1.21±0.02^{a}
5.	T4	7.67±0.08^{c}	6.18±0.02^{c}	6.8 ± 0.2^{b}	70.83±0.81^{b}	0.72±0.01^{a}	0.85±0.009^{b}	16.47±0.01^{a}	1.19±0.02^{a}
6.	T5	6.01±0.08^{d}	6.98±0.10^{d}	7.5 ± 0.1^{c}	75.98±1.23^{c}	0.77±0.01^{c}	0.86±0.002^{c}	10.46±0.08d	1.11±0.01^{c}
7.	T6	5.89±0.07^{d}	6.61±0.07^{e}	7.4 ± 0.2^{c}	75.21±0.82^{c}	0.70±0.01^{b}	0.84±0.01^{d}	16.66±0.08^{a}	1.20±0.01^{a}
8.	T7	6.82±0.08^{e}	6.39±0.1^{f}	7.2 ± 0.1^{b}	70.62±0.89^{b}	0.75±0.02^{a}	0.86±0.008^{e}	12.79±0.23^{b}	1.14±0.01^{d}
9.	T8	6.31±0.04^{f}	6.28±0.07^{f}	7.0 ± 0.2^{b}	70.51±1.09^{b}	0.74±0.01^{a}	0.86±0.004^{e}	13.45±0.74^{b}	1.13±0.02^{d}

The values with different superscript letters in a column are significantly different ($p < 0.05$).

degradation of polymeric chains, affecting the original polymer's molecular weight (Pillai et al., 2009; Roy et al., 2017). (Mohammadi et al., 2023) found contrasting results when comparing shrimp chitosan obtained via traditional and microwave-powered extracting methods. The research highlighted that the physico-chemical properties were notably affected by variations in heating process parameters. The traditional method produced heavy molecular weight chitosan with 12.7% yield, whereas microwave extraction produced medium molecular weight chitosan with a porous structure, yielding 11.8%. When microwave conditions were applied to conventional extraction, lesser molecular weight chitosan was obtained with the minimal yield of 10.8% and a reduced crystallinity index. Research conducted by Naznin, (2005) reported a moisture percentage ranging from 6.62 to 8.01% when employing various concentrations of the alkaline solution utilized in the deacetylation process. The research conducted out by Alishahi et al. (2011) indicated a moisture content of 2.5% in chitosan. The variance in these values may be attributed to the drying method employed in the current study, which involved sun drying for 6 h before oven drying. Implementing this approach could further decrease moisture percentage in both chitosan and chitin, resulting in a reduced moisture content. Chitosan extracted from fly pupae displayed a moisture content of 2.46%, which contributes to increased thermal stability. The lower moisture content inside polymeric chains attributed to the water molecules being adsorbed, resulting in a plasticizing impact on both thermal constancy as well as structure (Dehghannya & Ngadi, 2024). In contrast, chitosan sourced from shrimp (*Litopenaeus vannamei)* shells had a higher moisture content of 8.95% (Zapata-Luna et al., 2023). Chitosan exhibits significant hygroscopic properties because it can create hydrogen chains with water using both its amino and hydroxyl groups. Commercial powdered chitosan typically exhibits a moisture range of 5.89 to 7.86% (w/w), a factor found to be unaffected by the DD or molecular weight, as highlighted by Ssekatawa et al. (2021). In Ssekatawa et al. (2021) study, chitosan extracted from Ugandan edible mushrooms using traditional methods exhibited moisture content fluctuations of up to 6.4%. This variation may stem from the earliest moisture % of the fresh sample materials and the ecological factors during storage (Wang & Zhuang, 2022). Also, the powder compressibility is most significantly influenced by moisture content, as noted by Badwan et al. (2015). Elevated moisture content tends to reduce granule porosity and the likelihood of fragmentation, thereby enhancing granule strength, as explained by Tofiq et al. (2022). Findings from the research by Szymańska & Winnicka, (2015) intended that maintaining a low dewiness in chitosan, typically ranging from 6 to 10%, is crucial for enhancing its ability to form hydrogen bonding. Additionally, it was highlighted that a higher water content within the chitosan structure accelerates the polymer's degradation through hydrolysis reactions (Viljoen et al., 2014).

3.2. Solubility and pH

Solubility of chitosan performs a crucial function in evaluating the quality of chitosan obtained from either plant or animal sources. Greater solubility is indicative of higher purity and quality in the obtained chitosan (Bonilla et al., 2019). Chitosan's solubility can be impacted by various factors during the deacetylation of chitin, such as temperature, duration and alkali strength (El Knidri et al., 2018). For example, varying the heating duration and temperatures deacetylating chitin from same shrimp species using a consistent concentration of concentrated NaOH led to varying solubilities of consequent chitosan (de

Queiroz Antonino et al., 2017; Patria, 2013). From this Table 2 chitosan obtained from T5 treatment showed the best solubility (%) i.e. 75.98 ± 1.23%, however the solubility and pH content for T0 was obtained to be 59.04±0.03% and 6.6 ± 0.01 respectively. The observed variations in chitosan solubility in extraction could be attributed to a high DD and the optimal pH are the fundamental parameters intimidating solubility. In a separate study by Ssekatawa et al. (2021), chitosan derived from mushrooms showed moderate solubility ranging from 69% to 86% when extracted using traditional methods. This variation in solubility could be caused by the existence of inorganic minerals that were not entirely eliminated within demineralization, which significantly influenced solubility (Pellis et al., 2022). The solubility of chitosan, as documented in reviewed research papers ranges between 26.13% - 99.86% (Chen et al., 2022; Cheng et al., 2020; Zapata-Luna et al., 2023; Islam et al., 2019). When chitosan is disintegrated in acetic acid, it gains a positive charge through the protonation of inherent amino groups, forming NH^{+3}. With increasing pH, the amine groups lose their protonation, causing chitosan to lose its positive charge and become indissoluble starting from pH 6.5. Insolvability is evident in the visual appearance of chitosan solution, which turns cloudy (Zapata-Luna et al., 2023). Marine source chitosan such as crab, fish, and shrimp, crab and fish exhibited solubilities of 70%, 60% and 78% respectively. Moreover, solubility is dependent on the operational temperature during the deacetylation process, with increased temperatures leading to a reduction in solubility (S. Kumari et al., 2016). (Hossain & Iqbal, 2014) highlighted several key factors that affect solubility of chitosan, viewing temperature, duration of deacetylating, strength of alkali, ratio of chitin to basic solution and particle size. As per (Zhao et al., 2023), lesser solubleness of chitosan suggests insufficient process of deacetylation. The complete dissolvable property of chitosan relies on the reduction in the acetyl groups during deacetylating and a DD may potentially impact the results, as emphasized by Weißpflog et al. (2021).

Considering the influence of pH, as per (Aranaz et al., 2021)chitosan oligomers demonstrate solubleness throughout a wide pH spectrum, ranging between acidic to basic circumstances together with pH 7.4. pH of the mushroom debris derived chitosan in T5 treatment is 7.5 ± 0.1 closely aligning with the acceptable pH range for standard chitosan. Chitosan solutions tend to undergo phase separation when the pH exceeds 6.5, whereas solubility is observed at pH levels below 6.5. When in a soluble state, chitosan becomes positively charged because of having protonated amino groups (Elsabee et al., 2009). In solutions with a pH ranging from 6.0 to 6.5 the unbound amino groups in chitosan structure experience reduced protonation, leading to increased hydrophobicity along the chitosan chain. At pH levels below 6, chitosan chains have the capability to interact electrostatically with molecules or polymers that carry a negative charge such as anionic glycosamino glycans and proteoglycans. When the pH is elevated, exceeding approximately 6.5, the amino groups present in chitosan undergo deprotonation. This deprotonation can result in hydrophobic interactions between chitosan and various substrates, such as fatty acids and cholesterol, as exhibited in the research done by Dash et al. (2011). Chitosan is a substance characterized by its restricted solubility in water, alkaline solutions, and many commonly employed organic solutions. Nonetheless, it can partially solvable in diluted aqueous acid solutions, like diluted acetic acid (Inamdar & Mourya, 2014) (S. Kumari et al., 2016). In an aqueous acid solution, chitosan undergoes protonation because of the amino groups within its molecular framework which enhances its solubility (Inamdar & Mourya, 2014; Pillai et al., 2009; Roy et al., 2017) From the mentioned treatments, three treatments T2, T5 and T8 are selected on the basis of techno-functional properties like yield, moisture content, pH, solubility and flow properties. The T2, T5 and T8 treatments resulted more yield. Considering the flow properties, these treatments also offered insights good powder properties and good flowability indicating porous nature.

3.3. Degree of deacetylation (DD)

DA significantly impacts the quality of chitosan, with higher purity associated with an increased DD. Agarwal et al. (2018) observed that DD in chitosan varies relying on the variety and preparation technique, varying from 56% to 99%, with average around 80%. (Foster et al., 2015) defined chitosan as chitin having a DD more or equal to 75%. (Aldila et al., 2020) indicated that DD is persuaded by the strength of NaOH, highlighting the difficulty in removing acetyl groups bound in chitin. Thus, a considerable concentration of NaOH/KOH and elevated temperatures are required, as noted by (S. Kumari et al., 2017). This necessity stems from the significant influence of steric hindrance on the deacetylation process of chitin stemming from inherent chitin structure (Vicente et al., 2021). The hindrance caused by the dense structure of chitin inhibits the accessibility of OH- ions to attack the amino group. Moreover, the rate of diffusion OH- ions to both the outward and the interior of the chitin molecule is heavily reliant on the concentration of alkali (Aldila et al., 2020). Furthermore, the extent of deacetylation observed in commercial chitosan varies among 70% to 85%, as indicated by (Rasweefali et al., 2022). In our investigations, the DD of chitosan ranged among 75.09±0.34% to 79.94±0.13%, with the optimal outcome observed at a power level of 180 W in T5 (Table 3), The DD in the process of its production from mushroom waste is liable on various conditions. Studies have indicated that the DD tends to decrease with a rise in deproteinization temperature, a trend we also observed in our own research. In addition, using a traditional method, another mushroom species yielded chitosan having 78.1% DD. This DD value affects various properties of chitosan, including biological, physicochemical, and mechanical traits, as discussed by (Ssekatawa et al., 2021). The lower energy input into the system may have led to partial deacetylation of chitin, preventing it from fully solubilizing in an acidic medium (Pillai et al., 2009; Roy et al., 2017). Elevated-temperature processing adversely affects the DD of chitosan, as given by (Abdou et al., 2008), (Aldila et al., 2020) and (Cheng et al., 2020). In a separate investigation, (Yarnpakdee et al., 2022) documented DD values ranging among 73.56% to 75.56% for chitosan derived from aquatic mantis shrimp, which was constructed employing different deacetylation times (Zapata-Luna et al., 2023). Increasing the DD results in more amino groups being present in the C2 location of chitosan, leading to a greater plus charge and enhanced antimicrobial action (Thambiliyagodage et al., 2023). Nevertheless, deacetylation through acidic conditions and high temperatures is not the preferred method due to its detrimental impact on glycosidic bonds, polymer chain breakage, and the production of darker-colored chitosan. In contrast, gentler treatments result in chitosan with a lighter color, as observed in the findings of (Huq et al., 2022).

3.4. Crystallinity

The crystallinity of chitosan obtained using microwave methods is

Table 3
Effect of treatment on Degree of deacetylation, Crystallinity and bioactive properties of extracted chitosan samples.

S. No.	Chitosan sample	DD	CI	DPPH %	RP %
1.	T2	75.71 ±0.80^{ab}	1.06 ±0.12^{ab}	42.06 ±0.01^{a}	2.41% ±0.02^{a}
2.	T5	79.94 ±0.13^{c}	1.09±0.1^{a}	53.97 ±0.01^{c}	3.58 ±0.02^{c}
3.	T8	75.09 ±0.34^{b}	1.02±0.1^{c}	51.33 ±0.01^{b}	2.94 ±0.01^{b}

The values with different superscript letters in a column are significantly different ($p < 0.05$).
DD: Degree of deacetylation; CI: Crystallinity index; DPPH: 1,1-Diphenyl-2-picrylhydrazyl; RP: Reducing power.

outlined in Table 3. The crystallinity of chitosan produced in treatments T2, T5 and T8 are 1.06±0.12, 1.09±0.01 and 1.02±0.1 respectively. However, A notable correlation exist within DD and crystallinity of chitosan. The molecular chain of non-deacetylated chitin is comparatively consistent and demonstrates a high degree of chronicity, resulting in elevated crystallinity. Deacetylation induces diversity in the molecular chain, resulting in decreased crystallinity due to increased intermolecular hydrogen bonding and networking of polymer chains. Chitosan displays two primary peaks on the XRD diffractogram, typically occurring around 10° and 20° 2θ angle values. The initial peak corresponds to the 020 plane (amine I - acetylated amine group in chitosan), while the second peak is associated with the 110 plane (amine II - free amine group in chitosan). The 020 reflections are attributed to acetamide groups capable of forming hydrogen bonds with water, leading to the formation of hydrated crystals (Dziedzic et al., 2023). In research conducted by Agarwal et al. (2018), chitosan samples prepared using a traditional method exhibited a crystallinity index of 0.95. This was achieved by employing a 30% NaOH in a ratio of 1:50 (w/v) for extraction, followed by deacetylation under 15 psi pressure at 121 °C for 30 min following an autoclave. In this instance, the penetration of the NaOH solution amidst the α-chitin sequence may have been impeded by intermolecular network, resulting in a reduced DD in the sample. This method also exposes the sample to potential thermal and shear degradation common in conventional approaches. Microwave-assisted heating, however, could enhance our findings by promoting improved solvent mixing, which aids the penetration of solvents within the polysaccharide arrangement and facilitates the reaction (De Oliveira Silva et al., 2024). Nevertheless, with improved DD, the molecular chain has a tendency to homogenize, resulting in a corresponding rise in crystallinity (Lopes et al., 2021). During the reaction process, chitosan produced via microwave exhibited relatively high crystallinity, suggesting a more ordered arrangement of molecular chains. This indicates that microwave radiation could enhance the uniformity and completeness of the deacetylation reaction. Indeed, with a high DD, chitosan possesses fewer acetyl groups in its structure. Consequently, there is a reduction in intermolecular hydrogen bonding between hydroxyl and acetyl groups within its parallel arrangement, resulting in a lower degree of crystallinity (Nguyen et al., 2022).

3.5. Flow properties of mushroom waste chitosan

This research investigated the bulk density (BD) and tapped density (TD) along with carr's index, and Hausner ratio, to comprehend the rheological characteristics of isolated chitosan powders. Bulk and tapped density measurements offer insights into powder flowability. By utilizing both these values, the Carr's Index was determined, where a lower Carr's Index indicates improved powder flowability. Carr's values categorize flow properties into different ranges: 5 to 10 as excellent, 12 to 16 as good, 18 to 21 as fair, and 23 to 28 as poor (Azubuike et al., 2012). Conversely, for the Hausner ratio, a value below 1.20 shows beneficial flowability, while a value of 1.50 or above indicate deficient flow qualities. In this investigation, the chitosan extracted under T5 conditions (540W:180W:360 W) demonstrated Carr's index of 10.46 ±0.08 suggesting excellent or free-flowing features. The Hausner ratio for this sample was 1.11±0.01 which is underneath the threshold of 1.25 (demonstrating excellent flowability), additional verifying its favorable flow traits. For T0 lesser bulk and tapped density values are obtained ie., 0.67±0.04 and 0.83±0.02 however with respect to carr's index and hausner ratio the values are 19.27±0.04 and 1.24±0.03 respectively. The process of synthesis significantly influences the bulk, tapped, and packing characteristics of chitosan powders obtained from mushroom waste. Elevated bulk and tapped density may arise from minimal particulate irregularities, indicating a porous nature in the chitosan structure, as suggested by (Yarangsee et al., 2021). This could also imply that the chitosan has undergone a deproteinization treatment with a lower alkali concentration, as described by (Iber et al., 2022). Furthermore, the physico-chemical properties of chitosan T5 (540W:180W:360 W), derived through deacetylation from chitin in mushroom waste, closely resemble those of commercially sourced chitosan from shrimp shells or crab, as indicated in the literature. The obtained values for the Hausner ratio line up consistently with Carr's index. These results are consistent with the outcomes anticipated by Sreeharsha et al. (2024). In Olorunsola et al. (2017), chitosan extracted from shells of *Callinectes gladiator* using a traditional method exhibited a 62.7% DD along with 2.88 viscosity. The bulk density was measured at 0.60, with a tapped density of 0.74. Additionally, the % Carr's index was 18.90 and Hausner's ratio was 1.23. According to these measures, the chitosan exhibited acceptable flow characteristics and exhibited the maximum true density. True density, which excludes all void spaces, indicates the extent to which a powder can be compacted. Bulk density reflects a powder's compressibility—a lower bulk density suggests a greater tendency for densification, often due to particle irregularities and a porous structure (Taylor, 2021). The findings of our research aligned with those of (Iber et al., 2022). and (Iber et al., 2023), where bulk density mean value ranged among 0.19 to 0.28 g/mL, and tapped density dropped between 0.26 to 0.35 g/mL. An Improved bulk and tapped density of chitosan indicates greater porosity of the material (Iber et al., 2022). While chitosan from certain sequences in the current study may seem to have varying levels of porosity, the variation observed was not deemed significant. Another study involving the extraction of chitosan from giant freshwater prawns reported bulk and tapped densities of 0.25 g/mL and 0.32 g/mL, respectively, which aligns with the results of the present study (Iber et al., 2023).

3.6. Antioxidant activity (AA)

One important method of antioxidation involves scavenging hydrogen radicals. DPPH (2,2-diphenyl-1-picrylhydrazyl) has a hydrogen-free radical that absorbs light at 517 nm, which can be observed as the purple color of the solution. This color quickly fades when DPPH interacts with proton radical scavengers (Aradmehr & Javanbakht, 2020). The AA of chitosan produced in treatments T2, T5 and T8 are 42.06±0.01%, 53.97±0.01% and 51.33±0.01% (as shown in Table 3) respectively with the optimal outcome observed at a power level of 180 W in T5 having highest DD i.e., 79.94±0.13%. Ascorbic acid showed moderate to high scavenging abilities of 55.14%. The RP of respective chitosan samples shown in Table 3 at concentration of 1mg/ml showed moderate values of 2.41±0.02%, 3.58±0.02% and 2.94 ±0.01% for chitosan produced in treatments T2, T5 and T8. Thus, AA of chitosan was determined to be moderately effective at scavenging DPPH radicals. It appears that the scavenging abilities of chitosan improve as the DD increases.

These judgements align with the outcomes stated by (Samar et al., 2013) and where the chitosan from shrimp waste having DD range of 67.58–78.83%, 76.89–83.05% and 88.39–95.19% showed AA in the range of 16.14–20.54%, 21.27–25.18% and 21.03–32.76% at 1mg/ml, respectively. The scavenging capabilities of chitosan appear to enhance with higher DD due to the increased presence of amino groups on C2, which obstruct the oxidation of ascorbic acid, consequently boosting their AA. Current findings corroborate this hypothesis, indicating that the appearance of free amino groups plays a significant contribution in achieving effective antioxidant performance. Specifically, higher (DD) led to chitosan with improved antioxidant properties. Reducing power (RP) of chitosan samples at a concentration of 1mg/ml exhibited modest values (ranging from 1.87 to 2.28, 1.98 to 2.10, and 0.62 to 1.89) across the same chitosan samples. Another study highlighted the significance of extended deacetylation and its influence on scavenging action by generating highly deacetylated products (Avelelas et al., 2019). This study compared chitooligosaccharides (DD: 86−93%) with aqueous soluble chitosan (DD: 55−62%) and demonstrated that amino groups could be a significant factor in free radical scavenging action.

According to Kusnadi et al. (2022), after extracting white shrimp

(*Penaeus indicus*) chitosan, AA of the chitosan extract and commercial chitosan in scavenging DPPH radicals varied between 18.80% to 42.27% with a DD of 78.60%, and 13.45% to 33.86% having DD of 73.46%, respectively. Chitosan having improved DD has the potential for increased AA because of the higher concentration of amino compounds in its arrangement. Here AA can be correlated with maximum inhibitory concentration value (IC50). According to Chlif et al. (2021), a lower IC50 value indicates higher AA of the sample. The analysis results showed that the scavenging abilities of extracted chitosan, market based chitosan and ascorbic acid on DPPH radicals yielded IC50 values of 4.25 mg/mL, 5.2 mg/mL, and 1.45 mg/mL, separately. Similar positive correlation is shown by the results obtained by (Hafsa et al., 2016) upon extracting chitosan from *P. longirostris* shrimp shell chitosan indicated DD at 73.68% and 83.55% exhibited antioxidant values of 21.25% and 44.17%, respectively. Thus, it can be inferred that higher DD in chitosan leads to higher antioxidant values.

Earlier research has demonstrated that the AA of chitosan is substantially influenced by its DD (Román-Doval et al., 2023). This is attributed to the appearance of active hydroxyl and amino groups in chitosan chains, which can interact with unbound radicals (Wu et al., 2024) chitosan's capability to scavenge radicals may arise from the interaction between the unbound radicals and protonated amino groups as implied by (Harugade et al., 2023), Numerous researchers have proposed the scavenging action of chitosan which involves the interaction of hydroxyl and superoxide anion radicals with active hydrogen atoms in chitosan, resulting in the formation of a strong macromolecule radical. Within the chitosan molecule, at C − 2 (NH2), C − 3 (OH), and C − 6 (OH) positions are the main hydrogen origins as described by (Parameswaran et al., 2024).

3.7. Fourier transform infrared (FTIR) spectroscopy

The FTIR spectra of chitosan samples through various treatments is shown in Fig. 5. FTIR analysis of mushroom chitosan revealed distinct peaks that match the functional groups found in chitosan extracted from mushrooms. Chitosan exhibits distinct peaks at particular wave numbers that indicate its structural constituents. The FTIR spectra of chitosan display peaks, including O—H stretching peak typically ascertained in the range between 3200 and 3600 cm^{-1}. Peaks detected within the limits between 2850 and 3000 cm^{-1} signify the C—H expansion. Similarly, the existence of C = O stretching in Amide I is indicated by the appearance of peaks around 1650–1655 cm^{-1}, while the presence of N—H deflection in Amide II is indicated by peaks around 1595–1605 cm^{-1}. The existence of C—O-C expansion was displayed by the occurrence of vertices between 1060 and 1150. The peaks and intensities observed in mushroom chitosan deviated a little based against the treatment exerted, likely due to differences in molecular forms and derivation methods used. The analysis of the FTIR spectrum facilitated the identification of these distinctive functional groups and the verification of the molecular structure of chitosan.

The FTIR analysis exhibited the representative absorption peaks of T2 sample at the wavenumbers of 614 cm^{-1}, 1024, 1374 cm^{-1}, 1554 cm^{-1}, 1628 cm^{-1}, 2921 cm^{-1} and 3261 cm^{-1}. The absorption vertices of T5 sample were observed at 595 cm^{-1}, 1063 cm^{-1}, 1376 cm^{-1}, 1559 cm^{-1}, 1653 cm^{-1}, 2360 cm^{-1}, 2919 cm^{-1} and 3261 cm^{-1} wavenumbers. T8 sample displayed the characteristic absorption vertices at the wavenumbers of 843 cm^{-1}, 1024 cm^{-1}, 1448 cm^{-1}, 1649 cm^{-1} and 3262 cm^{-1}. An additional characteristic absorption peak was detected at wavenumber of ~ 2360 cm^{-1} in the case of the T5 sample while the characteristic peak observed at the wavenumber (2919 – 2921) cm^{-1} in the case of T2 and T5 samples was not detected in the T8 sample. Almost all the characteristic peaks observed in all the samples were similar except the aforementioned peaks. The shifting of the peaks in the higher wavenumbers with higher peak intensities was noted in T5 sample compared to the T2 and T8 samples which signifies better intra and intermolecular bonding of the T5 sample. Lowest characteristic absorption peak intensities detected in the case of the T8 samples could be ascribed to the weaker intra and intermolecular bonding frameworks. Thus, the FTIR analysis demonstrated the T5 sample as the better molecular bonding structure or the least affected one during the microwave-assisted extraction of mushroom chitosan.

The depiction of chitosan using FTIR derived results alike to those received in earlier analyses. Specifically, the stretching of the amide I band, attributed to the C = O group in chitosan retrieved from crayfish and shrimp, was found to be at 1660.41 cm^{-1} and 1658.48 cm^{-1} correspondingly. (Ossamulu et al., 2023). Whereas the peaks at the wavenumber 2918 cm^{-1} and 2921 cm^{-1} of the obtained *Agaricus bisporus* chitosan symbolizes the stretch vibration of CH_3 group as shown by (Shahadha et al., 2023). (Shahadha et al., 2023) also showed the Peaks at 1554 and 1559 cm^{-1}. The appearance of the vertice at around 1 in the relevant spectra indicates the N—H group in the second II amide bond. These findings regarding functional groups align with those reported by (Hadidi et al., 2020) where two peaks emerged at 1065 cm^{-1} approves the existence of C—O-C stretching. However similar results ratify the

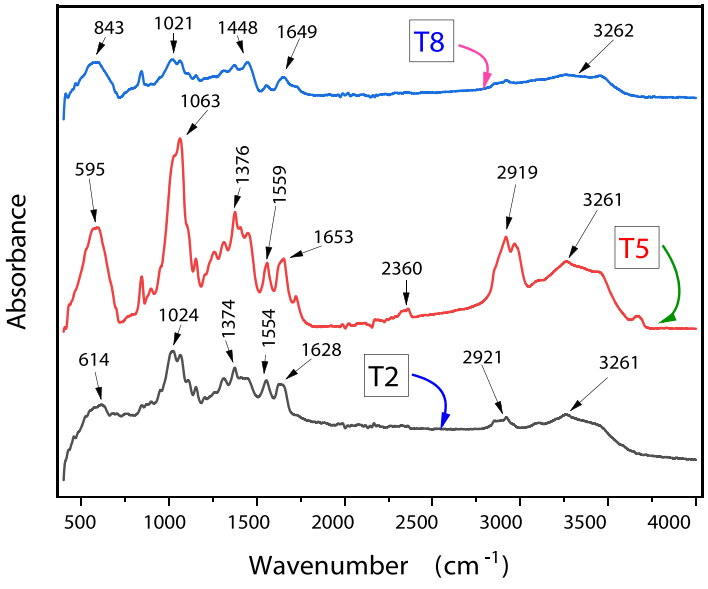

Fig. 5. FTIR spectra of chitosan samples obtained through various treatments.

existence of C—N stretching at 1350–1450 cm^{-1} by (Hadidi et al., 2020) where when diagnosing chitosan produced by FTIR device. Similar bands with comparable intensities are also noted nearly at 1550 and 1650 cm^{-1} in the chitosan spectrum, corresponding to the expansion vibrations of N—H and C═O (in the NHCOCH3 group) accordingly shown in the literature by (Da Silva Lucas et al., 2021). Similar FT-IR band with equivalent strength was also observed in the chitosan isolates from *C. echinulate*, the carbonyl stretching displayed frequency range of about 1643 and 1588 cm^{-1}. The peak observed at 1315–1320 cm^{-1} was assigned to the amide III bands. Two absorption bands at roughly 1655 as well as 1625 cm^{-1} are distinctive of amide groups that are hydrogen-bonded (Azeez et al., 2023). The findings corroborate previous reports regarding the production of chitosan from house cricket flour. Key functional groups like -NH and -OH bands, located near 3400 and 3300 cm^{-1} singly, were identified. Moreover, the spectrum showed the lengthening of the C = O bond at 1645 cm^{-1}, the deflection of the primary amine N—H bond at 1555 cm^{-1} and the expansion of the C—O bond corresponding to the five-carbon cyclic ether at approximately 1009 cm^{-1} (Espinosa-Solís et al., 2024). As mentioned in previous literature, characteristic bands in the regions of 1020–1065 cm^{-1} confirm the C—O expansion. Additionally, the band located near 890 cm^{-1} is attributed to the out-of-plane vibration of the C—H β-glycosidic bond (Martín-López et al., 2020; Wiercigroch et al., 2017). The lack of the band near 1540 cm^{-1} in the FTIR spectrum showed successful removal of proteins after deproteinization step. This particular band, which is attribute of N-acetyl groups and conforms the N—H twisting of amide-II, was hardly seen in our FTIR data, consistent with previous findings (Da Silva Lucas et al., 2021). Inside the fingerprint zone (600–1500 cm^{-1}), range 1147 and 1160 cm^{-1} exhibited sufficient absorbance intensity across all samples, demonstrating the lengthening of an asymmetric C–O bond and suggesting the existence of a glycosidic bonds among samples. depending on the wavenumbers observed, it could be inferred that all the extracted samples consist of chitosan (Lam et al., 2023). The peaks and intensities observed in mushroom chitosan showed slight variations relying on the treatment used. These differences possibly attributed to the distinct molecular framework and derivation techniques operated. The analysis of the FTIR spectrum enabled the recognition of these distinct functional band and the confirmation of the molecular structure of chitosan.

3.8. X-ray powder diffractometry (XRD)

The chitosan diffractogram obtained using three different treatments T8, T5 and T2 is shown in Fig. 6. The crystalline framework of mushroom-derived chitosan was assayed through X-ray diffraction (XRD), revealing the influence of extraction process. The X-ray diffraction (XRD) arrangement of mushroom chitosan exhibited distinct characteristics attributed to structural differences when equated to chitosan obtained from alternative sources. The XRD pattern can be swayed by factors like molecular weight, crystallinity and chitosan's purity derived from mushrooms. The impact of the extraction technique on the crystalline structure in these diffractograms was observed. Chitosan commonly displayed clear peaks in XRD as a result of its semi-crystalline characteristics. The primary peak attributed to chitosan was observed at 2θ values ranging from 10 to 20 °. The magnitude and location of this peak exhibited variations relying on the level of DD of chitosan, as well as its molecular mass. Examining the XRD graph entitles for the finding of the crystalline properties, level of crystallinity, and crystallographic structure of the chitosan obtained from mushrooms. The XRD curve showed a broad amorphous peak at 2θ value of 19.2° in all the samples. The crystalline peak of T2 was found to be at a 2θ value of 26.4 while at 26.0° for the T5 sample. The characteristic peaks of the T8 samples were observed the 2θ values of 26.3°, 29.4°, 32.3°, 33.5° and 37.8°. The peaks with improved crystallinity and larger peak intensities at the 2θ values of 29.4°, 32.3°, 33.5° and 37.8° of the T8 sample signified the more crystalline character compared to the remaining two (T2 and T5) samples. These peaks represent typical crystal patterns of α-chitin, which is the most prevalent type found in chitosan. The presence of these peaks is associated with ordered regions that involve the acetamide groups and hydrogen bonds (Lopes et al., 2021). The magnitude and location of this peak exhibited variations depends on DD of the chitosan and its molecular weight.

Rahayu et al. (2022) stated that these peaks are indicative of pure chitosan. However, the crystallinity index (CrI) of the chitosan got from these mushroom waste samples are lesser than the values documented in the literature. Ghasemi et al. (2021) observed that low values of the crystallinity index indicate an abundance of amorphous glucan within the chitin structure further indicating that the purity of mushroom chitosan extracted from *A. bisporous* waste is lower. Comparable diffraction peaks were detected for the exoskeleton of White shrimp (*Litopenneaus vannamei*) by (Martín-López et al., 2020). where crystalline planes at 2θ ≈ 19.7° can be attributed to origin of chitin Da Silva Lucas et al. (2021).

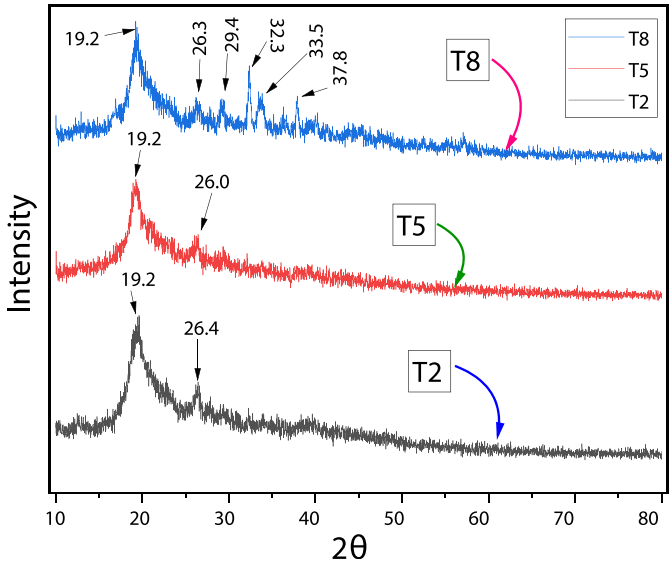

Fig. 6. Chitosan X-ray powder diffractometry obtained using three different treatments.

According to the literature, certain chitosan XRD formats show two distinct vertices, typically near 2θ ≈ 10° and 20°, as observed for chitosan obtained from *Agaricus bisporus* (Hassainia et al., 2018).The emergence has also been noted as DD rises as more steps are added during microwave extraction, indicating the presence of hydrated crystalline allomorphic chitosan (Martín-López et al., 2020). Comparable outcomes were also documented by Triunfo et al. (2022) and Tolesa et al. (2019), where chitin displayed prominent sharp peaks at 9° and 19°, along with 3 to 4 weaker peaks near 13°, 21°, 23° and 26°, depicting the α-form of the polymer. Equivalent representative vertices at 10.0 and 20.0 were disclosed in chitosan samples obtained from tiger shrimp supporting their chitosan nature with large difference in the strength of the XRD pattern throughout the orders. The level of deacetylation in chitosan determines its crystallinity. Chitosan is classified as fully crystalline when it reaches 100% DD, whereas any form with partial acetylation is categorized as semi-crystalline (Iber et al., 2023). The presence of crystallites within the amorphous zone of chitosan possible because of residual chitin that remains unreacted within the molecules (Tafi, 2022). Current investigation led by (Espinosa-Solís et al., 2024). a comparable XRD pattern was observed, exhibiting a similar form and location to those identified in the sample gained in this study. This confirms the distinctiveness of the compounds. Moreover, the presence of crystalline heights at approximately 9.6, 19.6, 21.1, and 23.7 ° in 2θ provides confirmation that the chitin derived is in the α-chitin form. Analyzing the XRD pattern enables the determination of the crystalline properties, level of crystallinity and crystallographic structure of the chitosan obtained from mushrooms.

3.9. Thermogravimetric analysis (TGA)

Outcome of TGA conducted on chitosan extracted from mushroom is demonstrated in Fig. 7. TGA results of chitosan derived from mushrooms demonstrated the variation in weight of the chitosan sample in relation to temperature. The curve exhibits indications of weight reduction occurring in three distinct phases. The initial phase of weight reduction, amounting to 13.61% of the total weight, takes place between 10 and 150 °C. At first, there was a little decrease in weight caused by the evaporation of moisture or volatile components in the chitosan sample. This phenomenon took place at lower temperatures. Next stage begins at around 150 °C and extends up to 350 °C with weight reduction of 48.08%. Hence, the primary deterioration transpired at elevated temperatures. During third stage, a significant weight loss of 38.03% within a temperature range of 350–450 °C occurred. This weight reduction is mostly because of breakdown of saccharides in the molecular structure of organic material and the subsequent final destruction of organic matter. The TGA curve exhibited a substantial reduction in weight, indicating the heat decomposition of the chitosan polymeric structure. Following the breakdown process, a residue bulk remained. The residue is composed of ash or non-volatile components that remain unaffected by the heating process. The contention is further supported by a residual percentage of 0.1372%, which confirms the absence of organic materials at temperatures above 500 °C suggests that the biopolymer does not contain any metal or inorganic components. The TGA curve yielded insights into the temperature stability and degradation behavior of the chitosan derived from mushrooms. TGA thermogram exhibited the three thermal decomposition phases of all the samples. The first stage occurred at ≤170 °C whereas the second and the third stages occurred at 201–500 °C and 500–800 °C separately.

Mass losses during the first stage were 12.9 %, 11.4 % and 24.1 % respectively for T2, T5 and T8 samples, which could be attributed to the moisture/water loss. The mass losses in the second stage were 55.4 %, 54.9 % and 57.3 % respectively for T2, T5 and T8 samples which can have assigned due to the chitosan degradation. The residual masses during the last stage of the thermal degeneration which was mainly inorganic material were 17.9 %, 19.8 % and 9.4 % for T2, T5 and T8 samples respectively. The relatively greater thermal stability of the T5 sample in the microwave-assisted extraction of mushroom chitosan was confirmed by the TGA curves of all samples. (Liyanage et al., 2022) obtained chitosan from white leg shrimp (*Litopenaeus vannamei*) with a thermal stability of 360 °C. The initial stage of degradation for both chitin and chitosan occurred between 30 and 100 °C, primarily because of the water disappearance from the samples. The subsequent stage of decomposition took place within the scope of 250–500 °C, resulting from the reduction of the saccharide framework of the molecules through evaporation or deamination processes. Another TGA curve displayed a comparable two-stage degradation pattern for chitosan, with an initial weight loss of 6.58% occurring at approximately 100 °C due to water removal. A significant weight reduction of 51.47% observed between 297 and 450 °C is attributed to the partitioning of chitosan and the breakdown of its amine group (Dalhatu et al., 2023). Similarly, Tolesa et al. (2019), depicted that the mass loss of shrimp shell chitosan occurred in three steps. In the first stage, a 3–5% mass loss was noted at temperatures around 120 °C due to the evaporation of water. Above 170 °C, the heat retention of ingrained chitin step by step drops, and its

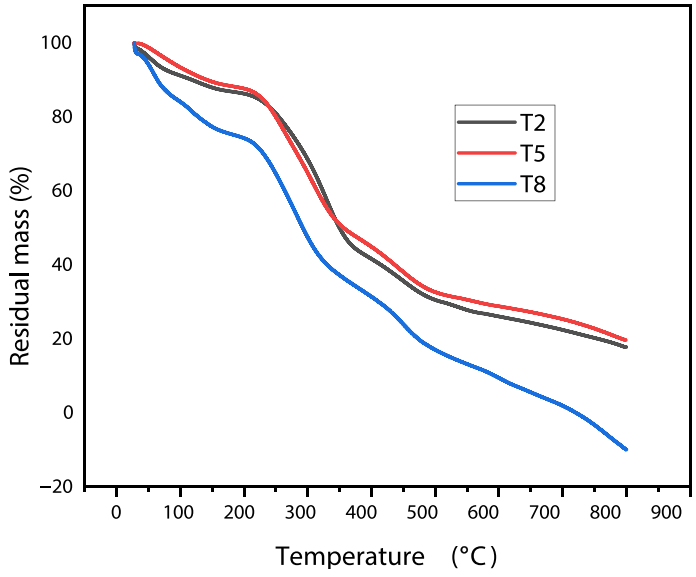

Fig. 7. Thermogravimetric analysis (TGA) of chitosan extracted from mushroom waste.

deterioration is completed at 441 °C. Moreover, the thermal profile of commercial α-chitin begins to decline at 267 °C and attain its decomposition at 406 °C. These results are steady with the results given by Ijaz et al. (2022), Huang et al. (2022) and Da Silva Lucas et al. (2021). Despite that this is linked to enhanced heat resistance for chitin. Following the deacetylation of chitin's branch chain, the order of crystalline level diminishes. Hence, the thermal resistance of the resulting chitosan is inferior to the original chitin. TGA spectra of chitosan extracted from mealworm cuticles exhibited similar thermograms, as presented in our study. It was noted that the thermogram of the polymer exhibits two primary stages of decomposition. The first decomposition occurs at 60–70 °C, leading to decrease in 11.1% of the earliest weight of both chitin and chitosan, followed by 70.9% at 210–270 °C, and was completely decomposed at nearly 400 °C. The TGA curve provided insights into the temperature stability and degradation behavior of the chitosan derived from mushrooms.

3.10. Differential scanning calorimetry (DSC)

DSC quantifies the transfer of heat (either into or out of) a sample in comparison to a reference material, with respect to temperature variations. Chitosan frequently undergoes a glass transition, transitioning from a amorphous form to a rubbery or viscous one. The transition temperature offered worthy insights concerning flexibility and mobility of the chitosan polymer chains. Chitosan can exhibit melting or crystallization peaks, which indicate changes between different solid states, depending on its purity and molecular structure. This knowledge is essential for comprehending its stability and prospective applications in controlled-release formulations or scaffold creation. DSC detected endothermic peaks associated with the liberation or uptake of moisture within the chitosan specimen. Differences in the DSC curve relative to pure chitosan may suggest modifications resulting from chemical changes or the use of additives during the extraction or processing of chitosan from mushrooms. The utilization of DSC for thermal study of low molecular weight chitosan, derived from mushrooms, revealed a broad endothermic peak in the temperature reach around 80–120 °C because of dehydration process of water.

Moreover, the observed rise in exothermic enthalpies of chitosan resulting from various treatments suggests variations in the molecules' intramolecular bonding strength, likely due to chain shortening. The To, Tm, Tc and ΔH of all the analyzed samples are shown in the Fig. 8. The To values were 59.8 °C, 65.0 °C and 91.0 for T2, T5 and T8 samples accordingly. Tm and Tc values were 82.4 °C, 87.5 °C and 99.1 °C; and 97.5 °C, 98.2 °C and 114.1 °C respectively for T2, T5 and T8 samples. ΔH values of all the samples were 0.046 *J*/g, 0.011 *J*/g and 0.791 respectively for T2, T5 and T8 samples. Higher values To, Tm, Tc and ΔH of the T8 samples indicated better thermal characteristics contrasted to the T5 and T2 samples. However, the concentration of NaOH employed in the deacetylation and deproteinization phases impacts the thermal stability of the samples. A gain in the strength of the NaOH results in a slender improvement in heat resistance. This observation is further supported by comparing the temperatures and heat change at the point of disintegration with those of market based chitosan (Soon et al., 2018). The application of DSC for thermal study of low molecular weight chitosan, derived from mushrooms, revealed a wide endothermic peak in the temperature reach of 87–100 °C, this process can be imputed to the dehydration process of water.

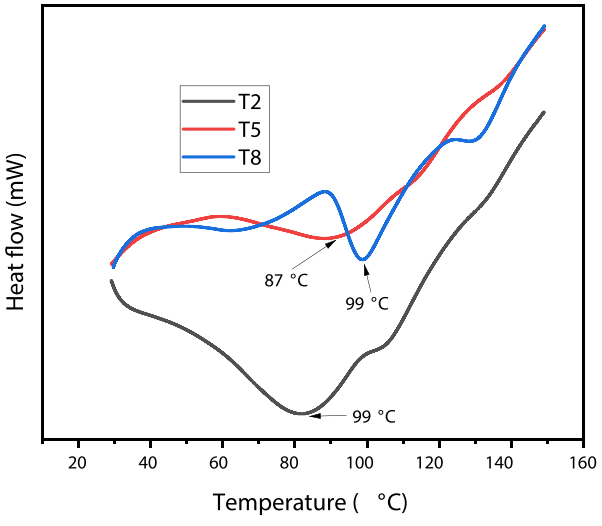

Fig. 8. Differential scanning calorimetry (DSC) of chitosan extracted from mushroom waste showing To, Tm, Tc and ΔH of all the samples.

According to Da Silva Lucas et al. (2021) market-based chitosan showed an exothermic having Tmax of 110.18 °C, akin to that discovered in chitosan extracted from mealworm's cuticles (111.96 °C). Above temperature drift is typical of the transition in the agglomeration phase, suggesting the removal of remained vapour within the sample, along with the initiation of material combustion as also noted in other studies (Hadidi et al., 2020; Ijaz et al., 2022; Molina-Ramírez et al., 2021). Likewise, thermogram derived from DSC analysis of chitosan extracted from cricket flour exhibits an exothermic rise at 185 °C, indicating the crystallization temperature (Tc). This suggests that the thermic aspects of chitosan align with its crystalline nature (Espinosa-Solís et al., 2024). In a different DSC thermogram of chitosan, two peaks are observed. The initial peak (endothermic, below 100 °C) is linked to the removal of the vapour. Second signal (exothermic, around 300 °C) is connected to the breakdown of the chitosan pyranose ring. The melting temperature of chitosan determined through DSC analysis is approximately 110 °C (Dziedzic et al., 2023). Thermal breakdown necessitates heat gain to disrupt hydrogen binding, a reaction recognized as an endothermic height, with the energy required for the reaction to happen. It is crucial to emphasize that for polysacharides melting situation (highest temperature) represents general melting point of crystallites. This is not a actual value for sample but quite rely on the molecular weight (Molina-Ramírez et al., 2021). Moreover, the observed rise in exothermic enthalpies of chitosan resulting from various treatments suggests variations in the molecules' intramolecular bonding strength, likely due to chain shortening.

4. Conclusion

The mushroom species, namely *A. bisporous*, produce significant amounts of waste, leading to appreciable yields of chitosan. However, if properly cultivated, mushrooms can become a dependable substitute origin for chitosan production in spite of primarily relying on aquatic sources. Techno-functional properties of the obtained chitosan demonstrate their viability as bio based polymers in biological system applications. Chitosan obtained using microwave heating reduces the deacetylation time (after two stages of weakening HCl solution for acid hydrolysis and diluting NaOH for deproteinization) from hours to just a few minutes (24 min), resulting in chitosan with a higher yield of 6.98% and improved degree of deacetylation up to 79.94% when compared to the traditional method. The current findings suggest that the extracted chitosan was solublize in a 1% acetic acid solution. The chitosan obtained during T5 treatment exhibited an optimal pH of 7.5, higher solubility up to 75% and a thicker crystalline configuration. This can be due to homogenization of the chitin molecular chain during deacetylation which tends to raises crystallinity accordingly. The extracted chitosan exhibited moisture content lower than 10% and ash content less than 1%, meeting the quality grade requirements for chitosan in various food and medical applications. With a maximum DPPH free radical scavenging activity of 53.97% at 1 mg/ml and a reducing power of 3.58% at 1 mg/ml, extracted chitosan (T5) demonstrates that chitosan's

scavenging capabilities get better as deacetylation increases. This clearly demonstrated that microwave assisted extraction of chitosan from mushroom waste is suitable for enhancing the antioxidant activity. The process of synthesis significantly influences the bulk, tapped, and packing characteristics of chitosan powders obtained from mushroom waste. The Carr's index of 10.46 for the chitosan extracted under T5 conditions indicated that it has good or free-flowing characteristics. This sample further demonstrated its excellent flow properties with a Hausner ratio of 1.11, which is below the threshold of 1.25 (showing remarkable flowability). Additionally, the Carr's index and Hausner ratio of 10.46 and 1.11 respectively for the chitosan extracted under T5 conditions indicated that it has good or free-flowing characteristics. This could also imply that the chitosan has undergone a deproteinization treatment with a lower alkali concentration. This eco-friendly safe method is significantly shorter, around sixteen times faster, than the conventional method, while still achieving the highest quality grade. This advancement opens up potential applications in medical and agricultural fields, including food packaging, pharmaceuticals, drug delivery systems, and water treatment.

Funding

Project No. TKP2021-NKTA-32 was implemented with support from the National Research, Development, and Innovation Fund of Hungary, financed under the TKP2021-NKTA funding scheme, and supported by the University of Debrecen Program for Scientific Publication.

List of abbreviations

DA- Degree of acetylation
DD- Degree of deacetylation
MWP- Mushroom waste powder
LDPE- Low density polyethylene
BD- Bulk density
AA- Antioxidant activity
DPPH- 2,2-diphenyl-1-picrylhydrazyl
RP- Reducing power
TD- Tapped density
FTIR- Fourier Transform Infrared Spectroscopy
CI- Crystallinity index
XRD- X-ray powder diffractometry
TGA- Thermogravimetric analysis
DSC- Differential scanning calorimetry

Data availability statement

The data supporting the outcomes of this research are available from the corresponding author against acceptable demand.

CRediT authorship contribution statement

Adity Bahndral: Writing – original draft, Validation, Software, Resources, Methodology, Investigation, Formal analysis, Data curation, Conceptualization. **Rafeeya Shams:** Writing – review & editing, Writing – original draft, Validation, Supervision, Software, Resources, Methodology, Investigation, Funding acquisition, Formal analysis, Data curation, Conceptualization. **Kshirod Kumar Dash:** Writing – review & editing, Writing – original draft, Visualization, Validation, Supervision, Software, Resources, Project administration, Methodology, Investigation, Funding acquisition, Formal analysis, Data curation, Conceptualization. **Pintu Chaudhary:** Visualization, Validation, Software, Investigation. **Ayaz Mukarram Shaikh:** Writing – review & editing, Visualization, Validation, Software, Investigation, Funding acquisition. **Kovács Béla:** Writing – review & editing, Validation, Software, Project administration, Methodology, Investigation, Funding acquisition, Formal analysis.

Declaration of competing interest

The authors declare that they have no known competing financial interests or personal relationships that could have appeared to influence the work reported in this paper.

Data availability

Data will be made available on request.

References

Abdel-Gawad, K. M., Hifney, A. F., Fawzy, M. A., & Gomaa, M. (2017). Technology optimization of chitosan production from Aspergillus niger biomass and its functional activities. *Food Hydrocolloids, 63*, 593–601. https://doi.org/10.1016/j.foodhyd.2016.10.001

Abdou, E. S., Nagy, K. S. A., & Elsabee, M. Z. (2008). Extraction and characterization of chitin and chitosan from local sources. *Bioresource Technology, 99*(5), 1359–1367. https://doi.org/10.1016/j.biortech.2007.01.051

Abolhasani, M., & Kumacheva, E. (2023). The rise of self-driving labs in chemical and materials sciences. *Nature Synthesis*. https://doi.org/10.1038/s44160-022-00231-0

Abourehab, M. A. S., Pramanik, S., Abdelgawad, M. A., Abualsoud, B. M., Kadi, A., Ansari, M. J., & Deepak, A. (2022). Recent advances of chitosan formulations in biomedical applications. *International Journal of Molecular Sciences, 23*(18), 10975. https://doi.org/10.3390/ijms231810975

Agarwal, M., Agarwal, M. K., Shrivastav, N., Pandey, S., & Gaur, P. (2018). A simple and effective method for preparation of chitosan from chitin. *Int. J. Life. Sci. Sci. Res, 41*, 721–1728. https://doi.org/10.21276/ijlssr.2018.4.2.18

Aldila, H., Asmar, Fabiani, V. A., Dalimunthe, D. Y., & Irwanto, R. (2020). The effect of deproteinization temperature and NaOH concentration on deacetylation step in optimizing extraction of chitosan from shrimp shells waste. *IOP Conference Series. Earth and Environmental Science, 599*(1), Article 012003. https://doi.org/10.1088/1755-1315/599/1/012003

Alishahi, A., Mirvaghefi, A., Tehrani, M. R., Farahmand, H., Shojaosadati, S. A., Dorkoosh, F. A., & Elsabee, M. Z. (2011). Enhancement and characterization of chitosan extraction from the wastes of shrimp packaging plants. *Journal of Polymers and the Environment, 19*(3), 776–783. https://doi.org/10.1007/s10924-011-0321-5

Aradmehr, A., & Javanbakht, V. (2020). A novel biofilm based on lignocellulosic compounds and chitosan modified with silver nanoparticles with multifunctional properties: Synthesis and characterization. *Colloids and Surfaces. A, Physicochemical and Engineering Aspects, 600*(124952), Article 124952. https://doi.org/10.1016/j.colsurfa.2020.124952

Aranaz, I., Alcántara, A. R., Civera, M. C., Arias, C., Elorza, B., Heras Caballero, A., & Acosta, N. (2021). Chitosan: An overview of its properties and applications. *Polymers, 13*(19), 3256. https://doi.org/10.3390/polym13193256

Avelelas, F., Horta, A., Pinto, L. F. V., Cotrim Marques, S., Marques Nunes, P., Pedrosa, R., & Leandro, S. M. (2019). Antifungal and antioxidant properties of chitosan polymers obtained from nontraditional Polybius henslowii sources. *Marine Drugs, 17*(4), 239. https://doi.org/10.3390/md17040239

Azeez, S., Sathiyaseelan, A., Jeyaraj, E. R., Saravanakumar, K., Wang, M.-H., & Kaviyarasan, V. (2023). Extraction of chitosan with different physicochemical properties from Cunninghamella echinulata (Thaxter) Thaxter for biological applications. *Applied Biochemistry and Biotechnology, 195*(6), 3914–3927. https://doi.org/10.1007/s12010-022-03982-w

Azubuike, C. P., & Okhamafe, A. O. (2012). Physicochemical, spectroscopic and thermal properties of microcrystalline cellulose derived from corn cobs. *International journal of recycling of organic waste in agriculture, 1*, 1–7. https://doi.org/10.1186/2251-7715-1-9

Badwan, A. A., Rashid, I., Omari, M. M. H. A., & Darras, F. H. (2015). Chitin and chitosan as direct compression excipients in pharmaceutical applications. *Marine Drugs, 13*(3), 1519–1547. https://doi.org/10.3390/md13031519

Banik, B. K., Sahoo, B. M., Kumar, B. V. V. R., Panda, K. C., Jena, J., Mahapatra, M. K., & Borah, P. (2021). Green synthetic approach: An efficient Eco-friendly tool for synthesis of biologically active oxadiazole derivatives. *Molecules (Basel, Switzerland), 26*(4), 1163. https://doi.org/10.3390/molecules26041163

Bhagarathi, L. K., Subramanian, G., & Dasilva, P. N. (2023). A review of mushroom cultivation and production, benefits and therapeutic potentials. *World Journal of Biology Pharmacy and Health Sciences, 15*(2), 1–056. https://doi.org/10.30574/wjbphs.2023.15.2.0333

Bonilla, F., Chouljenko, A., Lin, A., Young, B. M., Goribidanur, T. S., Blake, J. C., Bechtel, P. J., & Sathivel, S. (2019). Chitosan and water-soluble chitosan effects on refrigerated catfish fillet quality. *Food Bioscience, 31*(100426), Article 100426. https://doi.org/10.1016/j.fbio.2019.100426

Boureghda, Y., Satha, H., & Bendebane, F. (2021). Chitin-glucan complex from Pleurotus ostreatus mushroom: Physicochemical characterization and comparison of extraction methods. *Waste Biomass Valorization, 12*, 6139–6153. https://doi.org/10.1007/s12649-021-01449-3

Chen, Q., Qi, Y., Jiang, Y., Quan, W., Luo, H., Wu, K., Li, S., & Ouyang, Q. (2022). Progress in research of chitosan chemical modification technologies and their applications. *Marine Drugs, 20*(8), 536. https://doi.org/10.3390/md20080536

Cheng, J., Zhu, H., Huang, J., Zhao, J., Yan, B., Ma, S., Zhang, H., & Fan, D. (2020). The physicochemical properties of chitosan prepared by microwave heating. *Food Science & Nutrition, 8*(4), 1987–1994. https://doi.org/10.1002/fsn3.1486

Chlif, N., Ed-Dra, A., Diouri, M., El Messaoudi, N., Zekkori, B., Filali, F. R., & Bentayeb, A. (2021). Chemical composition, antibacterial and antioxidant activities of essential oils extracted from dry and fresh Brocchia cinerea (Vis). *Biodiversitas Journal of Biological Diversity, 22*(4). https://doi.org/10.13057/biodiv/d220418

Cummings, R. D. (2024). Evolution and diversity of glycomolecules from unicellular organisms to humans. *BioCosmos: New perspectives on the origin and evolution of life, 4*(1), 1–35. https://doi.org/10.2478/biocosmos-2024-0001

Da Costa, A. A. F., De Oliveira, A. D. N., Esposito, R., Auvigne, A., Len, C., & Luque, R. (2023). Glycerol and microwave-assisted catalysis: recent progress in batch and flow devices. *Sustainable Energy & Fuels, 7*(8), 1768–1792. https://doi.org/10.1039/D2SE01647H

Da Silva Lucas, A. J., Oreste, E. Q., Costa, H. L. G., López, H. M., Saad, C. D. M., & Prentice, C. (2021). Extraction, physicochemical characterization, and morphological properties of chitin and chitosan from cuticles of edible insects. *Food Chemistry*. https://doi.org/10.1016/j.foodchem.2020.128550

Dai, D., Qv, M., Liu, D., Tang, C., Wang, W., Wu, Q., Yin, Z., & Zhu, L. (2023). Structural insights into mechanisms of rapid harvesting of microalgae with pH regulation by magnetic chitosan composites: A study based on E-DLVO model and component fluorescence analysis. *Chemical Engineering Journal (Lausanne, Switzerland: 1996), 456*(141071), Article 141071. https://doi.org/10.1016/j.cej.2022.141071

Dalhatu, S. N., Modu, K. A., Mahmoud, A. A., Zango, Z. U., Umar, A. B., Usman, F., … Aldaghri, O. A. (2023). L-arginine grafted chitosan as corrosion inhibitor for mild steel protection. *Polymers, 15*(2), 398. https://doi.org/10.3390/polym15020398

Dash, M., Chiellini, F., Ottenbrite, R. M., & Chiellini, E. (2011). Chitosan—A versatile semi-synthetic polymer in biomedical applications. *Progress in polymer science, 36*(8), 981–1014. https://doi.org/10.1016/j.progpolymsci.2011.02.001

De Oliveira Silva, M. B., De Oliveira, S. A., & Rosa, D. (2024). Comparative study on microwave-assisted and conventional chitosan production from shrimp shell: Process optimization, characterization, and environmental impacts. *Journal of Cleaner Production, 440*, Article 140726. https://doi.org/10.1016/j.jclepro.2024.140726

de Queiroz Antonino, R. S. C. M., Lia Fook, B. R. P., de Oliveira Lima, V. A., de Farias Rached, R.Í., Lima, E. P. N., da Silva Lima, R. J., Peniche Covas, C. A., & Lia Fook, M. V. (2017). Preparation and characterization of chitosan obtained from shells of shrimp (Litopenaeus vannamei Boone). *Marine Drugs, 15*(5). https://doi.org/10.3390/md15050141

Dehghannya, J., & Ngadi, M. (2024). The application of glass transition temperature in the frying of starchy foods: A review. *Food Reviews International, 40*(7), 1980–1998. https://doi.org/10.1080/87559129.2023.2245030

Duan, M., Sun, J., Yu, S., Zhi, Z., Pang, J., & Wu, C. (2023). Insights into electrospun pullulan-carboxymethyl chitosan/PEO core-shell nanofibers loaded with nanogels for food antibacterial packaging. *International Journal of Biological Macromolecules, 233*(123433), Article 123433. https://doi.org/10.1016/j.ijbiomac.2023.123433

Dziedzic, I., & Kertmen, A. (2023). Methods of chitosan identification: history and trends. *Lett. Appl. NanoBioSci, 12*, 94. https://doi.org/10.33263/LIANBS124.094

Egorov, A. R., Kirichuk, A. A., Rubanik, V. V., Rubanik, V. V., Jr, Tskhovrebov, A. G., & Kritchenkov, A. S (2023). Chitosan and its derivatives: Preparation and antibacterial properties. *Materials, 16*(18). https://doi.org/10.3390/ma16186076

El Knidri, H., Belaabed, R., Addaou, A., Laajeb, A., & Lahsini, A. (2018). Extraction, chemical modification and characterization of chitin and chitosan. *International Journal of Biological Macromolecules, 120*(Pt A), 1181–1189. https://doi.org/10.1016/j.ijbiomac.2018.08.139

El Knidri, H., El Khalfaouy, R., Laajeb, A., Addaou, A., & Lahsini, A. (2016). Eco-friendly extraction and characterization of chitin and chitosan from the shrimp shell waste via microwave irradiation. *Process Safety and Environmental Protection: Transactions of the Institution of Chemical Engineers, Part B,, 104*, 395–405. https://doi.org/10.1016/j.psep.2016.09.020

El Sheikha, A. F. (2022). Nutritional profile and health benefits of Ganoderma lucidum "Lingzhi, reishi, or mannentake" as functional foods: Current scenario and future perspectives. *Foods (Basel, Switzerland), 11*(7), 1030. https://doi.org/10.3390/foods11071030

Elsabee, M. Z., Morsi, R. E., & Al-Sabagh, A. M. (2009). Surface active properties of chitosan and its derivatives. *Colloids and Surfaces. B, Biointerfaces, 74*(1), 1–16. https://doi.org/10.1016/j.colsurfb.2009.06.021

Espinosa-Solís, A., Velázquez-Segura, A., Lara-Rodríguez, C., Martínez, L. M., Chuck-Hernández, C., & Rodríguez-Sifuentes, L. (2024). Optimizing chitin extraction and chitosan production from house cricket flour. *Processes (Basel, Switzerland), 12*(3), 464. https://doi.org/10.3390/pr12030464

Feng, L., Liu, H., Li, L., Wang, X., Kitazawa, H., & Guo, Y. (2022). Improving the property of a reproducible bioplastic film of glutenin and its application in retarding senescence of postharvest Agaricus bisporus. *Food Bioscience, 48*(101796), Article 101796. https://doi.org/10.1016/j.fbio.2022.101796

Foster, L. J. R., Ho, S., Hook, J., Basuki, M., & Marçal, H. (2015). Chitosan as a biomaterial: Influence of degree of deacetylation on its physiochemical, material and biological properties. *PloS One, 10*(8), Article e0135153. https://doi.org/10.1371/journal.pone.0135153

Ghassemi, N., Poulhazan, A., Deligey, F., Mentink-Vigier, F., Marcotte, I., & Wang, T. (2021). Solid-state NMR investigations of extracellular matrixes and cell walls of algae, bacteria, fungi, and plants. *Chemical Reviews, 122*(10), 10036–10086. https://doi.org/10.1021/acs.chemrev.1c00669

Gichuki, J., Kareru, P. G., Gachanja, A. N., & Ngamau, C. (2022). Characteristics of microcrystalline cellulose from coir fibers. *Journal of Natural Fibers, 19*(3), 915–930. https://doi.org/10.1080/15440478.2020.1764441

González, A., Cruz, M., Losoya, C., Nobre, C., Loredo, A., Rodríguez, R., Contreras, J., & Belmares, R. (2020). Edible mushrooms as a novel protein source for functional foods. *Food & Function, 11*(9), 7400–7414. https://doi.org/10.1039/d0fo01746a

Hadidi, M., Pouramin, S., Adinepour, F., Haghani, S., & Jafari, S. M. (2020). Chitosan nanoparticles loaded with clove essential oil: Characterization, antioxidant and antibacterial activities. *Carbohydrate Polymers, 236*(116075), Article 116075. https://doi.org/10.1016/j.carbpol.2020.116075

Hafsa, J., Smach, M. A., Charfeddine, B., Limem, K., Majdoub, H., & Rouatbi, S. (2016). Antioxidant and antimicrobial proprieties of chitin and chitosan extracted from Parapenaeus Longirostris shrimp shell waste. *Annales Pharmaceutiques Francaises, 74*(1), 27–33. https://doi.org/10.1016/j.pharma.2015.07.005

Harugade, A., Sherje, A. P., & Pethe, A. (2023). Chitosan: A review on properties, biological activities and recent progress in biomedical applications. *Reactive and Functional Polymers, 191*, Article 105634. https://doi.org/10.1016/j.reactfunctpolym.2023.105634

Hassainia, A., Satha, H., & Boufi, S. (2018). Chitin from Agaricus bisporus: Extraction and characterization. *International Journal of Biological Macromolecules, 117*, 1334–1342. https://doi.org/10.1016/j.ijbiomac.2017.11.172

Hisham, F., Maziati Akmal, M. H., Ahmad, F., Ahmad, K., & Samat, N. (2024). Biopolymer chitosan: Potential sources, extraction methods, and emerging applications. *Ain Shams Engineering Journal, 15*(2), Article 102424. https://doi.org/10.1016/j.asej.2023.102424

Hossain, M. S., & Iqbal, A. (2014). Production and characterization of chitosan from shrimp waste. *Journal of the Bangladesh Agricultural University, 12*(1), 153–160. https://doi.org/10.3329/jbau.v12i1.21405

Hu, Q., He, Y., Wang, F., Wu, J., Ci, Z., Chen, L., Xu, R., Yang, M., Lin, J., Han, L., & Zhang, D. (2021). Microwave technology: a novel approach to the transformation of natural metabolites. *Chinese Medicine, 16*(1), 87. https://doi.org/10.1186/s13020-021-00500-8

Huang, W.-C., Zhao, D., Xue, C., & Mao, X. (2022). An efficient method for chitin production from crab shells by a natural deep eutectic solvent. *Marine Life Science & Technology, 4*(3), 384–388. https://doi.org/10.1007/s42995-022-00129-y

Huq, T., Khan, A., Brown, D., Dhayagude, N., He, Z., & Ni, Y. (2022). Sources, production and commercial applications of fungal chitosan: A review. *Journal of Bioresources and Bioproducts, 7*(2), 85–98. https://doi.org/10.1016/j.jobab.2022.01.002

Iber, B. T., Torsabo, D., Chik, C. E. N. C. E., Wahab, F., Abdullah, S. R. S., Hasan, H. A., & Kasan, N. A. (2023). Optimization of chitosan coagulant from dry legs of giant freshwater prawn, Macrobrachium rosenbergii in aquaculture wastewater treatment using response surface methodology (RSM). *Journal of Environmental Chemical Engineering, 11*(3), Article 109761. https://doi.org/10.1016/j.jece.2023.109761

Iber, B. T., Torsabo, D., Chik, C. E. N. C. E., Wahab, F., Abdullah, S. R. S., Hassan, H. A., & Kasan, N. A. (2022). The impact of re-ordering the conventional chemical steps on the production and characterization of natural chitosan from biowaste of Black Tiger Shrimp, Penaeus monodon. *Journal of Sea Research, 190*(102306), Article 102306. https://doi.org/10.1016/j.seares.2022.102306

Ibitoye, E. B., Lokman, I. H., Hezmee, M. N. M., Goh, Y. M., Zuki, A. B. Z., & Jimoh, A. A. (2018). Extraction and physicochemical characterization of chitin and chitosan isolated from house cricket. *Biomedical Materials (Bristol, England), 13*(2), Article 025009. https://doi.org/10.1088/1748-605x/aa9dde

Ijaz, H., Tulain, U. R., Minhas, M. U., Mahmood, A., Sarfraz, R. M., Erum, A., & Danish, Z. (2022). Design and in vitro evaluation of pH-sensitive crosslinked chitosan-grafted acrylic acid copolymer (CS-co-AA) for targeted drug delivery. *International Journal of Polymeric Materials, 71*(5), 336–348. https://doi.org/10.1080/00914037.2020.1833011

Inamdar, N. N., & Mourya, V. (2014). Chitosan and low molecular weight chitosan: Biological and biomedical applications. *Advanced Biomaterials and Biodevices* (pp. 183–242). John Wiley & Sons, Inc. https://doi.org/10.1002/9781118774052.ch6

Islam, A., Islam, M. S., Zakaria, M. U. M. A., Paul, S. C., & Mamun, A. A. (2019). Extraction and worth evaluation of chitosan from shrimp and prawn co-products. *American Journal of Food Technology, 15*(1), 43–48. https://doi.org/10.3923/ajft.2020.43.48

Jindal, M., Kumar, V., Rana, V., & Tiwary, A. K. (2013). Exploring potential new gum source Aegle marmelos for food and pharmaceuticals: Physical, chemical and functional performance. *Industrial Crops and Products, 45*, 312–318. https://doi.org/10.1016/j.indcrop.2012.12.037

Khubiev, O. M., Egorov, A. R., Kirichuk, A. A., Khrustalev, V. N., Tskhovrebov, A. G., & Kritchenkov, A. S. (2023). Chitosan-based antibacterial films for biomedical and food applications. *International Journal of Molecular Sciences, 24*(13). https://doi.org/10.3390/ijms241310738

Korampattu, L., Ghosh, N., & Dhepe, P. L. (2024). Shell waste valorization to chemicals: methods and progress. *Green Chemistry: An International Journal and Green Chemistry Resource: GC, 26*(10), 5601–5634. https://doi.org/10.1039/d3gc05177c

Kritchenkov, A. S., Zhaliazniak, N. V., Egorov, A. R., Lobanov, N. N., Volkova, O. V., Zabodalova, L. A., Suchkova, E. P., Kurliuk, A. V., Shakola, T. V., Rubanik, V. V., Jr, Rubanik, V. V., Yagafarov, N. Z., Khomik, A. S., & Khrustalev, V. N (2020). Chitosan derivatives and their based nanoparticles: ultrasonic approach to the synthesis, antimicrobial and transfection properties. *Carbohydrate Polymers, 242*(116478), Article 116478. https://doi.org/10.1016/j.carbpol.2020.116478

Kumari, S., Kumar Annamareddy, S. H., Abanti, S., & Kumar Rath, P. (2017). Physicochemical properties and characterization of chitosan synthesized from fish scales, crab and shrimp shells. *International Journal of Biological Macromolecules, 104*(Pt B), 1697–1705. https://doi.org/10.1016/j.ijbiomac.2017.04.119

Kumari, S., Rath, P., & Kumar, A. S. H. (2016). Chitosan from shrimp shell (Crangon crangon) and fish scales (Labeorohita): Extraction and characterization Suneeta. *African Journal of Biotechnology, 15*(24), 1258–1268. https://doi.org/10.5897/AJB2015.15138

Kusnadi, K., Purgiyanti, P., Kumoro, A. C., & Legowo, A. M. (2022). The antioxidant and antibacterial activities of chitosan extract from white shrimp shell (Penaeus indicus) in the waters north of Brebes, Indonesia. *Biodiversitas: Journal of Biological Diversity, 23*(3). https://doi.org/10.13057/biodiv/d230310

Lam, I. L. J., Mohd Affandy, M. A., Aqilah, N. M. N., Vonnie, J. M., Felicia, W. X. L., & Rovina, K. (2023). Physicochemical characterization and antimicrobial analysis of vegetal chitosan extracted from distinct forest fungi species. *Polymers, 15*(10). https://doi.org/10.3390/polym15102328

Liaqat, F., Xu, L., Khazi, M. I., Ali, S., Rahman, M. U., & Zhu, D. (2023). Extraction, purification, and applications of vanillin: A review of recent advances and challenges. *Industrial Crops and Products, 204*(117372), Article 117372. https://doi.org/10.1016/j.indcrop.2023.117372

Liu, M., Zhou, Y., Zhang, Y., Yu, C., & Cao, S. (2013). Preparation and structural analysis of chitosan films with and without sorbitol. *Food Hydrocolloids, 33*(2), 186–191. https://doi.org/10.1016/j.foodhyd.2013.03.003

Liyanage, C. S., Gonapinuwala, S. T., Fernando, C. A. N., & De Croos, M. D. S. T. (2022). Physico-chemical properties of chitosan extracted from Whiteleg shrimp (Litopenaeus vannamei) processing shell waste in Sri Lanka. *Sri Lanka Journal of Aquatic Sciences, 27*(2), 107. https://doi.org/10.4038/sljas.v27i2.7600

Lopes, I. S., Michelon, M., Duarte, L. G. R., Prediger, P., Cunha, R. L., & Picone, C. S. F. (2021). Effect of chitosan structure modification and complexation to whey protein isolate on oil/water interface stabilization. *Chemical Engineering Science, 230* (116124), Article 116124. https://doi.org/10.1016/j.ces.2020.116124

Mahdy, S. (2019). Optimization of Microwave technique conditions for Shrimp chitin deacetylation by response surface methodology. *Journal of Bioscience and Applied Research, 5*(1), 75–91. https://doi.org/10.21608/jbaar.2019.109402

Malm, M. (2021). *Doctoral dissertation*. Purdue University.

Manna, S., Seth, A., Gupta, P., Nandi, G., Dutta, R., Jana, S., & Jana, S. (2023). Chitosan derivatives as carriers for drug delivery and biomedical applications. *ACS Biomaterials Science & Engineering, 9*(5), 2181–2202. https://doi.org/10.1021/acsbiomaterials.2c01297

Maray, A. R. M., Mostafa, M. K., & El-Fakhrany, A. E.-D. M. A. (2018). Effect of pretreatments and drying methods on physico-chemical, sensory characteristics and nutritional value of oyster mushroom. *Journal of Food Processing and Preservation, 42* (1), e13352. https://doi.org/10.1111/jfpp.13352

Martín-López, H., Pech-Cohuo, S. C., Herrera-Pool, E., Medina-Torres, N., Cuevas-Bernardino, J. C., Ayora-Talavera, T., Espinosa-Andrews, H., Ramos-Díaz, A., Trombotto, S., & Pacheco, N. (2020). Structural and physicochemical characterization of chitosan obtained by UAE and its effect on the growth inhibition of Pythium ultimum. *Agriculture, 10*(10), 464. https://doi.org/10.3390/agriculture10100464

Mohammadi, P., Taghavi, E., Foong, S. Y., Rajaei, A., Amiri, H., de Tender, C., Peng, W., Lam, S. S., Aghbashlo, M., Rastegari, H., & Tabatabaei, M. (2023). Comparison of shrimp waste-derived chitosan produced through conventional and microwave-assisted extraction processes: Physicochemical properties and antibacterial activity assessment. *International Journal of Biological Macromolecules, 242*(Pt 2), Article 124841. https://doi.org/10.1016/j.ijbiomac.2023.124841

Molina-Ramírez, C., Mazo, P., Zuluaga, R., Gañán, P., & Álvarez-Caballero, J. (2021). Characterization of chitosan extracted from fish scales of the Colombian endemic species Prochilodus magdalenae as a novel source for antibacterial starch-based films. *Polymers, 13*(13), 2079. https://doi.org/10.3390/polym13132079

Naznin, R. (2005). Extraction of chitin and chitosan from shrimp (Metapenaeus monoceros) shell by chemical method. *Pakistan Journal of Biological Sciences: PJBS, 8* (7), 1051–1054. https://doi.org/10.3923/pjbs.2005.1051.1054

Nguyen, H. T.-T., Tran, T. N., Ha, A. C., & Huynh, P. D (2022). Impact of deacetylation degree on properties of chitosan for formation of electrosprayed nanoparticles. *Journal of Nanotechnology, 2022*, 1–11. https://doi.org/10.1155/2022/2288892

Novikov, V. Y., Derkach, S. R., Konovalova, I. N., Dolgopyatova, N. V., & Kuchina, Y. A. (2023). Mechanism of heterogeneous alkaline deacetylation of chitin: a review. *Polymers, 15*(7), 1729. https://doi.org/10.3390/polym15071729

Olorunsola, E. O., Adedokun, M. O., & Akpabio, E. I. (2017). Evaluation of Callinectes chitosan as a superdisintegrant in metronidazole tablet. *International Journal of Pharmacy and Pharmaceutical Sciences, 9*(10), 111. https://doi.org/10.22159/ijpps.2017v9i10.20788

Omer, A. M., Khalifa, R. E., Tamer, T. M., Elnouby, M., Hamed, A. M., Ammar, Y. A., Ali, A. A., Gouda, M., & Eldin, M. S. M. (2019). Fabrication of a novel low-cost superoleophilic nonanyl chitosan-poly (butyl acrylate) grafted copolymer for the adsorptive removal of crude oil spills. *International Journal of Biological Macromolecules, 140*, 588–599. https://doi.org/10.1016/j.ijbiomac.2019.08.169

Ossamulu, F., Evbouan, S., Akanya, H., Egwim, E., & Zobeashia, S. L.-T. (2023). Characterization of chitosan extracted from three mushroom species from Edo State, Nigeria. *Ovidius University Annals of Chemistry, 34*(1), 22–27. https://doi.org/10.2478/auoc-2023-0004

Pandey, R., Pandey, V. S., & Pandey, V. N. (2024). Nutraceutical metabolites, value addition and industrial products for developing entrepreneurship through edible fleshy fungi. *Entrepreneurship with microorganisms* (pp. 293–328). Academic Press. https://doi.org/10.1016/B978-0-443-19049-0.00010-4

Papoutsis, K., Grasso, S., Menon, A., Brunton, N. P., Lyng, J. G., Jacquier, J. C., & Bhuyan, D. J. (2020). Recovery of ergosterol and vitamin D2 from mushroom waste-Potential valorization by food and pharmaceutical industries. *Trends in Food Science & Technology, 99*, 351–366. https://doi.org/10.1016/j.tifs.2020.03.005

Parameswaran, K. R., Suhaimin, N. S., & Jaafar, J. (2024). Chitosan incorporated with titanium (IV) oxide membrane for direct methanol fuel cell application. *Journal of Applied Membrane Science & Technology, 28*(1), 73–90. https://doi.org/10.11113/amst.v28n1.288

Pasanphan, W., Rattanawongwiboon, T., Choofong, S., Güven, O., & Katti, K. K. (2015). Irradiated chitosan nanoparticle as a water-based antioxidant and reducing agent for a green synthesis of gold nanoplatforms. *Radiation Physics and Chemistry (Oxford, England: 1993), 106*, 360–370. https://doi.org/10.1016/j.radphyschem.2014.08.023

Patria, A. (2013). Production and characterization of Chitosan from shrimp shells waste. *Aquaculture, Aquarium, Conservation & Legislation, 6*(4), 339–344. Microsoft Word - 2013.339-344.doc.

Pellis, A., Guebitz, G. M., & Nyanhongo, G. S. (2022). Chitosan: sources, processing and modification techniques. *Gels, 8*(7), 393. https://doi.org/10.3390/gels8070393

Pérez-Bassart, Z., Reyes, A., Martínez-Abad, A., López-Rubio, A., & Fabra, M. J. (2023). Feasibility of Agaricus bisporus waste biomass to develop biodegradable food packaging materials. *Food Hydrocolloids, 142*, Article 108861. https://doi.org/10.1016/j.foodhyd.2023.108861

Pillai, C. K. S., Paul, W., & Sharma, C. P. (2009). Chitin and chitosan polymers: Chemistry, solubility and fiber formation. *Progress in Polymer Science, 34*(7), 641–678. https://doi.org/10.1016/j.progpolymsci.2009.04.001

Rahangdale, D., Joshi, N., & Kumar, A. (2019). Chitosan and its derivatives: A new versatile biopolymer for various applications. *Functional Chitosan* (pp. 1–42). Singapore: Springer. https://doi.org/10.1007/978-981-15-0263-7_1

Rahayu, A. P., Islami, A. F., Saputra, E., Sulmartiwi, L., Rahmah, A. U., & Kurnia, K. A. (2022). The impact of the different types of acid solution on the extraction and adsorption performance of chitin from shrimp shell waste. *International Journal of Biological Macromolecules, 194*, 843–850. https://doi.org/10.1016/j.ijbiomac.2021.11.137

Raman, J., Lee, S. K., Im, J. H., Oh, M. J., Oh, Y. L., & Jang, K. Y. (2018). Current prospects of mushroom production and industrial growth in India. *Journal of Mushroom, 16*(4), 239–249. https://doi.org/10.14480/JM.2018.16.4.239

Rasweefali, M. K., Sabu, S., Muhammed Azad, K. S., Raseel Rahman, M. K., Sunooj, K. V., Sasidharan, A., & Anoop, K. K. (2022). Influence of deproteinization and demineralization process sequences on the physicochemical and structural characteristics of chitin isolated from Deep-sea mud shrimp (Solenocera hextii). *Advances in Biomarker Sciences and Technology, 4*, 12–27. https://doi.org/10.1016/j.abst.2022.03.001

Román-Doval, R., Torres-Arellanes, S. P., Tenorio-Barajas, A. Y., Gómez-Sánchez, A., & Valencia-Lazcano, A. A. (2023). Chitosan: Properties and its application in agriculture in context of molecular weight. *Polymers, 15*(13), 2867. https://doi.org/10.3390/polym15132867

Roy, J. C., Salaün, F., Giraud, S., Ferri, A., Chen, G., & Guan, J. (2017). Solubility of chitin: Solvents, solution behaviors and their related mechanisms. *Solubility of Polysaccharides*. InTech. https://doi.org/10.5772/intechopen.71385

Samar, M. M., El-Kalyoubi, M. H., Khalaf, M. M., & El-Razik, M. M. (2013). Physicochemical, functional, antioxidant and antibacterial properties of chitosan extracted from shrimp wastes by microwave technique. *Annals of Agricultural Sciences, 58*(1), 33–41. https://doi.org/10.1016/j.aoas.2013.01.006

Sebastian, J., Rouissi, T., Brar, S. K., Hegde, K., & Verma, M. (2019). Microwave-assisted extraction of chitosan from Rhizopus oryzae NRRL 1526 biomass. *Carbohydrate Polymers, 219*, 431–440. https://doi.org/10.1016/j.carbpol.2019.05.047

Shahadha, A. F., Al-Aubadi, I. M., & Merzah, N. R. (2023). Preparation of chitosan from agaricus bisporus brown stems and studying some its physicochemical and functional properties. In *IOP conference series: earth and environmental science*. IOP Publishing. https://doi.org/10.1016/j.aoas.2013.01.006. Vol. 1259.

Shoueir, K. R., El-Desouky, N., Rashad, M. M., Ahmed, M. K., Janowska, I., & El-Kemary, M. (2021). Chitosan based-nanoparticles and nanocapsules: Overview, physicochemical features, applications of a nanofibrous scaffold, and bioprinting. *International Journal of Biological Macromolecules, 167*, 1176–1197. https://doi.org/10.1016/j.ijbiomac.2020.11.072

Silva, M., Ramos, A. C., Lidon, F. J., Reboredo, F. H., & Gonçalves, E. M. (2024). Pre-and postharvest strategies for pleurotus ostreatus mushroom in a circular economy approach. *Circular Economy Approach. Foods, 13*(10). https://doi.org/10.3390/foods13101464

Singh, I., & Thakur, P. (2023). Impact of fungi on the world economy and its sustainability: Current status and potentials. *Fungal resources for sustainable economy: current status and future perspectives* (pp. 3–37). Springer Nature. https://doi.org/10.1007/978-981-19-9103-5_1

Siwulski, M., Budka, A., Rzymski, P., Gąsecka, M., Kalač, P., Budzyńska, S., Magdziak, Z., Niedzielski, P., Mleczek, P., & Mleczek, M. (2020). Worldwide basket survey of multielemental composition of white button mushroom Agaricus bisporus. *Chemosphere, 239*(124718), Article 124718. https://doi.org/10.1016/j.chemosphere.2019.124718

Soon, C. Y., Tee, Y. B., Tan, C. H., Rosnita, A. T., & Khalina, A. (2018). Extraction and physicochemical characterization of chitin and chitosan from Zophobas morio larvae in varying sodium hydroxide concentration. *International Journal of Biological Macromolecules, 108*, 135–142. https://doi.org/10.1016/j.ijbiomac.2017.11.138

Sreeharsha, N., Gajula, L. R., Srikruthi, K. S., Bhavani, P. D., Goudanavar, P., Rakshitha, A., … Sreenivasalu, P. K. P. (2024). Enhancing flowability of lamivudine through quasi-emulsion solvent-diffusion (QESD) crystallization: A comprehensive study on surfactant impact, particle morphology by QbD concepts and tablet compression challenges. *European Journal of Pharmaceutical Sciences*. , Article 106835. https://doi.org/10.1016/j.ejps.2024.106835

Ssekatawa, K., Byarugaba, D. K., Wampande, E. M., Moja, T. N., Nxumalo, E., Maaza, M., Sackey, J., Ejobi, F., & Kirabira, J. B. (2021). Isolation and characterization of chitosan from Ugandan edible mushrooms, Nile perch scales and banana weevils for biomedical applications. *Scientific Reports, 11*(1), 4116. https://doi.org/10.1038/s41598-021-81880-7

Szymańska, E., & Winnicka, K. (2015). Stability of chitosan-a challenge for pharmaceutical and biomedical applications. *Marine Drugs, 13*(4), 1819–1846. https://doi.org/10.3390/md13041819

Tafi, E. (2022). *Doctoral dissertation*. University of Basilicata.

Taylor, K. M. (2021). *Aulton's pharmaceutics E-book: Aulton's pharmaceutics, The design and manufacturer of medicines* (pp. 172–183), 6(1).

Thakur, M. P. (2020). Advances in mushroom production: Key to food, nutritional and employment security: A review. *Indian Phytopathology, 73*(3), 377–395. https://doi.org/10.1007/s42360-020-00244-9

Thambiliyagodage, C., Jayanetti, M., Mendis, A., Ekanayake, G., Liyanaarachchi, H., & Vigneswaran, S. (2023). Recent advances in chitosan-based applications—A review. *Materials, 16*(5), 2073. https://doi.org/10.3390/ma16052073

Thirugnanasambandan, T., & Gopinath, S. C. B. (2023). Laboratory to industrial scale synthesis of chitosan-based nanomaterials: A review. *Process Biochemistry (Barking, London, England), 130*, 147–155. https://doi.org/10.1016/j.procbio.2023.04.008

Tofiq, M., Nordström, J., Persson, A.-S., & Alderborn, G. (2022). Deciphering the role of granule deformation and fragmentation for the tableting performance of some dry granulated powders. *Powder Technology, 409*(117794), Article 117794. https://doi.org/10.1016/j.powtec.2022.117794

Tolesa, L. D., Gupta, B. S., & Lee, M.-J. (2019). Chitin and chitosan production from shrimp shells using ammonium-based ionic liquids. *International Journal of Biological Macromolecules, 130*, 818–826. https://doi.org/10.1016/j.ijbiomac.2019.03.018

Triunfo, M., Tafi, E., Guarnieri, A., Salvia, R., Scieuzo, C., Hahn, T., Zibek, S., Gagliardini, A., Panariello, L., Coltelli, M. B., De Bonis, A., & Falabella, P. (2022). Characterization of chitin and chitosan derived from Hermetia illucens, a further step in a circular economy process. *Scientific Reports, 12*(1), 6613. https://doi.org/10.1038/s41598-022-10423-5

Vetter, J. (2007). Chitin content of cultivated mushrooms Agaricus bisporus, Pleurotus ostreatus and Lentinula edodes. *Food Chemistry, 102*(1), 6–9. https://doi.org/10.1016/j.foodchem.2006.01.037

Vicente, F. A., Huš, M., Likozar, B., & Novak, U. (2021). Chitin deacetylation using deep eutectic solvents: Ab initio-supported process optimization. *ACS Sustainable Chemistry & Engineering, 9*(10), 3874–3886. https://doi.org/10.1021/acssuschemeng.0c08976

Viljoen, J. M., Steenekamp, J. H., Marais, A. F., & Kotzé, A. F. (2014). Effect of moisture content, temperature and exposure time on the physical stability of chitosan powder and tablets. *Drug Development and Industrial Pharmacy, 40*(6), 730–742. https://doi.org/10.3109/03639045.2013.782501

Wang, J., & Zhuang, S. (2022). Chitosan-based materials: Preparation, modification and application. *Journal of Cleaner Production, 355*(131825), Article 131825. https://doi.org/10.1016/j.jclepro.2022.131825

Wattjes, J., Sreekumar, S., Richter, C., Cord-Landwehr, S., Singh, R., El Gueddari, N. E., & Moerschbacher, B. M. (2020). Patterns matter part 1: Chitosan polymers with non-random patterns of acetylation. *Reactive and Functional Polymers, 151*, Article 104583. https://doi.org/10.1016/j.reactfunctpolym.2020.104583

Weißpflog, J., Vehlow, D., Müller, M., Kohn, B., Scheler, U., Boye, S., & Schwarz, S. (2021). Characterization of chitosan with different degree of deacetylation and equal viscosity in dissolved and solid state-Insights by various complimentary methods. *International Journal of Biological Macromolecules, 171*, 242–261. https://doi.org/10.1016/j.ijbiomac.2021.01.010

Wiercigroch, E., Szafraniec, E., Czamara, K., Pacia, M. Z., Majzner, K., Kochan, K., Kaczor, A., Baranska, M., & Malek, K. (2017). Raman and infrared spectroscopy of carbohydrates: A review. *Spectrochimica Acta. Part A, Molecular and Biomolecular Spectroscopy,, 185*, 317–335. https://doi.org/10.1016/j.saa.2017.05.045

Wu, L., Xie, X., Huang, J., He, J., & Liu, F. (2024). Preparation of chitosan-based macromolecular synergistic antioxidants containing hindered phenolic and secondary amine structures and its effects on thermo-oxidative aging of styrene-butadiene rubber/silica composites. *Polymers for Advanced Technologies, 35*(5). https://doi.org/10.1002/pat.6426

Yadav, K. K., Krishnan, S., Gupta, N., Prasad, S., Amin, M. A., Cabral-Pinto, M. M. S., Sharma, G. K., Marzouki, R., Jeon, B.-H., Kumar, S., Singh, N., Kumar, A., Rezania, S., & Islam, S. (2021). Review on evaluation of renewable bioenergy potential for sustainable development: Bright future in energy practice in India. *ACS Sustainable Chemistry & Engineering, 9*(48), 16007–16030. https://doi.org/10.1021/acssuschemeng.1c03114

Yarangsee, C., Wattanaarsakit, P., Sirithunyalug, J., & Leesawat, P. (2021). Particle engineering of chitosan and kaolin composite as a novel tablet excipient by nanoparticles formation and co-processing. *Pharmaceutics, 13*(11), 1844. https://doi.org/10.3390/pharmaceutics13111844

Yarnpakdee, S., Kaewprachu, P., Jaisan, C., Senphan, T., Nagarajan, M., & Wangtueai, S. (2022). Extraction and physico-chemical characterization of chitosan from mantis shrimp (Oratosquilla nepa) shell and the development of bio-composite film with agarose. *Polymers, 14*(19), 3983. https://doi.org/10.3390/polym14193983

Yu, M., Zhang, K., Guo, X., & Qian, L. (2023). Effects of the degree of deacetylation on the single-molecule mechanics of chitosans. *The Journal of Physical Chemistry. B, 127*(19), 4261–4267. https://doi.org/10.1021/acs.jpcb.3c01661

Zapata-Luna, R. L., Davidov-Pardo, G., Pacheco, N., Ayora-Talavera, T., Espinosa-Andrews, H., García-Márquez, E., & Cuevas-Bernardino, J. C. (2023). Structural and physicochemical properties of bio-chemical chitosan and its performing in an active film with quercetin and Phaseolus polyanthus starch. *Revista Mexicana de Ingeniería Química, 22*(2), 1–7. https://doi.org/10.24275/rmiq/Alim2315

Zhan, Z., Feng, Y., Zhao, J., Qiao, M., & Jin, Q. (2024). Valorization of seafood waste for food packaging development. *Foods (Basel, Switzerland), 13*(13), 2122. https://doi.org/10.3390/foods13132122

Zhang, Z., Song, H., Peng, Z., Luo, Q., Ming, J., & Zhao, G. (2012). Characterization of stipe and cap powders of mushroom (Lentinus edodes) prepared by different grinding methods. *Journal of Food Engineering, 109*(3), 406–413. https://doi.org/10.1016/j.jfoodeng.2011.11.007

Zhao, J.-Y., Hong, T., Hou, Y.-J., Song, X.-X., Yin, J.-Y., Geng, F., & Nie, S.-P. (2023). Comparison of structures and emulsifying properties between water-extracted pectins from Fructus aurantii. *International Journal of Biological Macromolecules, 242*(Pt 3), Article 125005. https://doi.org/10.1016/j.ijbiomac.2023.125005

Zion Market Research, N. Y. (2021). *Button Mushroom Market Size, Scope, Analysis 2028*.